5. Garrett, W. S., G. M. Lord, S. Punit, G. Lugo-Villarino, S. K. Mazmanian, S. Ito, J. N. Glickman, and L. H. Glimcher. 2007. Communicable ulcerative colitis induced by T-bet deficiency in the innate immune system. *Cell* 131: 33–45.
6. Kosmaczewska, A., L. Ciszak, S. Potoczek, and I. Frydecka. 2008. The significance of Treg cells in defective tumor immunity. *Arch. Immunol. Ther. Exp. (Warsz.)* 56: 181–191.
7. Markowitz, S., J. Wang, L. Myeroff, R. Parsons, L. Sun, J. Lutterbaugh, R. S. Fan, E. Zborowska, K. W. Kinzler, B. Vogelstein, et al. 1995. Inactivation of the type II TGF-beta receptor in colon cancer cells with microsatellite instability. *Science* 268: 1336–1338.
8. Takaku, K., M. Oshima, H. Miyoshi, M. Matsui, M. F. Seldin, and M. M. Taketo. 1998. Intestinal tumorigenesis in compound mutant mice of both Dpc4 (Smad4) and Apc genes. *Cell* 92: 645–656.
9. Kim, B. G., C. Li, W. Qiao, M. Mamura, B. Kasprzak, M. Anver, L. Wolfraim, S. Hong, E. Mushinski, M. Potter, et al. 2006. Smad4 signalling in T cells is required for suppression of gastrointestinal cancer. *Nature* 441: 1015–1019.
10. Shi, M. J., and J. Stavnezer. 1998. CBF alpha3 (AML2) is induced by TGF-beta1 to bind and activate the mouse germline Ig alpha promoter. *J. Immunol.* 161: 6751–6760.
11. Zhang, Y., and R. Derynck. 2000. Transcriptional regulation of the transforming growth factor-beta -inducible mouse germ line Ig alpha constant region gene by functional cooperation of Smad, CREB, and AML family members. *J. Biol. Chem.* 275: 16979–16985.
12. Pardali, E., X. Q. Xie, P. Tsapogas, S. Itoh, K. Arvanitidis, C. H. Heldin, P. ten Dijke, T. Grundström, and P. Sideras. 2000. Smad and AML proteins synergistically confer transforming growth factor beta1 responsiveness to human germline IgA genes. *J. Biol. Chem.* 275: 3552–3560.
13. Hanai, J., L. F. Chen, T. Kanno, N. Ohtani-Fujita, W. Y. Kim, W. H. Guo, T. Imamura, Y. Ishidou, M. Fukuchi, M. J. Shi, et al. 1999. Interaction and functional cooperation of PEBP2/CBF with Smads. Synergistic induction of the immunoglobulin germline Calpha promoter. *J. Biol. Chem.* 274: 31577–31582.
14. Taniuchi, I., M. Osato, T. Egawa, M. J. Sunshine, S. C. Bae, T. Komori, Y. Ito, and D. R. Littman. 2002. Differential requirements for Runx proteins in CD4 repression and epigenetic silencing during T lymphocyte development. *Cell* 111: 621–633.
15. Sato, T., S. Ohno, T. Hayashi, C. Sato, K. Kohu, M. Satake, and S. Habu. 2005. Dual functions of Runx proteins for reactivating CD8 and silencing CD4 at the commitment process into CD8 thymocytes. *Immunity* 22: 317–328.
16. Ohno, S., T. Sato, K. Kohu, K. Takeda, K. Okumura, M. Satake, and S. Habu. 2008. Runx proteins are involved in regulation of CD122, Ly49 family and IFN-gamma expression during NK cell differentiation. *Int. Immunol.* 20: 71–79.
17. Kohu, K., T. Sato, S. Ohno, K. Hayashi, R. Uchino, N. Abe, M. Nakazato, N. Yoshida, T. Kikuchi, Y. Iwakura, et al. 2005. Overexpression of the Runx3 transcription factor increases the proportion of mature thymocytes of the CD8 single-positive lineage. *J. Immunol.* 174: 2627–2636.
18. Fainaru, O., E. Woolf, J. Lotem, M. Yarmus, O. Brenner, D. Goldenberg, V. Negreanu, Y. Bernstein, D. Levanon, S. Jung, and Y. Groner. 2004. Runx3 regulates mouse TGF-beta-mediated dendritic cell function and its absence results in airway inflammation. *EMBO J.* 23: 969–979.
19. Watanabe, K., M. Sugai, Y. Nambu, M. Osato, T. Hayashi, M. Kawaguchi, T. Komori, Y. Ito, and A. Shimizu. 2010. Requirement for Runx proteins in IgA class switching acting downstream of TGF-beta 1 and retinoic acid signaling. *J. Immunol.* 184: 2785–2792.
20. Li, Q. L., K. Ito, C. Sakakura, H. Fukamachi, K. Inoue, X. Z. Chi, K. Y. Lee, S. Nomura, C. W. Lee, S. B. Han, et al. 2002. Causal relationship between the loss of RUNX3 expression and gastric cancer. *Cell* 109: 113–124.
21. Ito, K., A. C. Lim, M. Salto-Tellez, L. Motoda, M. Osato, L. S. Chuang, C. W. Lee, D. C. Voon, J. K. Koo, H. Wang, et al. 2008. RUNX3 attenuates beta-catenin/T cell factors in intestinal tumorigenesis. *Cancer Cell* 14: 226–237.
22. Brenner, O., D. Levanon, V. Negreanu, O. Golubkov, O. Fainaru, E. Woolf, and Y. Groner. 2004. Loss of Runx3 function in leukocytes is associated with spontaneously developed colitis and gastric mucosal hyperplasia. *Proc. Natl. Acad. Sci. USA* 101: 16016–16021.
23. Morita, S., T. Kojima, and T. Kitamura. 2000. Plat-E: an efficient and stable system for transient packaging of retroviruses. *Gene Ther.* 7: 1063–1066.
24. Gonda, H., M. Sugai, Y. Nambu, T. Katakai, Y. Agata, K. J. Mori, Y. Yokota, and A. Shimizu. 2003. The balance between Pax5 and Id2 activities is the key to AID gene expression. *J. Exp. Med.* 198: 1427–1437.
25. Asseman, C., S. Mauze, M. W. Leach, R. L. Coffman, and F. Powrie. 1999. An essential role for interleukin 10 in the function of regulatory T cells that inhibit intestinal inflammation. *J. Exp. Med.* 190: 995–1004.
26. Gondek, D. C., L. F. Lu, S. A. Quezada, S. Sakaguchi, and R. J. Noelle. 2005. Cutting edge: contact-mediated suppression by CD4+CD25+ regulatory cells involves a granzyme B-dependent, perforin-independent mechanism. *J. Immunol.* 174: 1783–1786.
27. Bruno, L., L. Mazzarella, M. Hoogenkamp, A. Hertweck, B. S. Cobb, S. Sauer, S. Hadjur, M. Leleu, Y. Naoe, J. C. Telfer, et al. 2009. Runx proteins regulate Foxp3 expression. *J. Exp. Med.* 206: 2329–2337.
28. Rudra, D., T. Egawa, M. M. Chong, P. Treuting, D. R. Littman, and A. Y. Rudensky. 2009. Runx-CBFbeta complexes control expression of the transcription factor Foxp3 in regulatory T cells. *Nat. Immunol.* 10: 1170–1177.
29. Klunker, S., M. M. Chong, P. Y. Mantel, O. Palomares, C. Bassin, M. Ziegler, B. Rückert, F. Meiler, M. Akdis, D. R. Littman, and C. A. Akdis. 2009. Transcription factors RUNX1 and RUNX3 in the induction and suppressive function of Foxp3+ inducible regulatory T cells. *J. Exp. Med.* 206: 2701–2715.
30. Kitoh, A., M. Ono, Y. Naoe, N. Ohkura, T. Yamaguchi, H. Yaguchi, I. Kitabayashi, T. Tsukada, T. Nomura, Y. Miyachi, et al. 2009. Indispensable role of the Runx1-Cbfbeta transcription complex for in vivo-suppressive function of FoxP3+ regulatory T cells. *Immunity* 31: 609–620.
31. Ono, M., H. Yaguchi, N. Ohkura, I. Kitabayashi, Y. Nagamura, T. Nomura, Y. Miyachi, T. Tsukada, and S. Sakaguchi. 2007. Foxp3 controls regulatory T-cell function by interacting with AML1/Runx1. *Nature* 446: 685–689.

PROSPECT
Journal of Cellular Biochemistry 112:409–414 (2011)

Journal of Cellular Biochemistry

Functions of Runx in IgA Class Switch Recombination

Manabu Sugai,* Kakeru Watanabe, Yukiko Nambu, Tatsunari Hayashi, and Akira Shimizu

Translational Research Center, Kyoto University Hospital, 54 Shogoin-Kawahara-cho, Sakyo-ku, Kyoto 606-8507, Japan

ABSTRACT

Runt-related (*Runx*) transcriptional regulators play essential roles in various cell fate determination processes, and dysfunction of these regulators causes many human diseases. Considerable insight into the functions of Runx proteins was provided mainly by studies of hematopoietic and skeletal disorders. Recently, extensive investigations have revealed new functions of these transcription factors in immune cell differentiation and functioning. In the present review, we discuss the mechanisms of selective IgA production in the intestine and report the involvement of Runx proteins in this process. J. Cell. Biochem. 112: 409–414, 2011. © 2010 Wiley-Liss, Inc.

KEY WORDS: RUNX; IGA; CLASS SWITCH RECOMBINATION; GERMLINE TRANSCRIPTION; INTESTINE

Runt-related (*Runx*) genes are evolutionarily conserved transcription factors that determine cell fate by regulating lineage-specific gene expression. Three *Runx* genes have been reported in mammals; *Runx1* plays a key role in definitive hematopoiesis and is frequently involved in the pathogenesis of human leukemia [Okuda et al., 1996; Wang et al., 1996; Osato, 2004; Chen et al., 2009], *Runx2* is essential for bone development [Komori et al., 1997; Otto et al., 1997] and haploinsufficiency of it causes cleidcranial displasia, and *Runx3* is a tumor suppressor involved in gastric cancer [Li et al., 2002]. In addition, *Runx3* has more widespread regulatory roles in the differentiation and functioning of various cell types, including T cells [Taniuchi et al., 2002; Kohu et al., 2005; Sato et al., 2005], dendritic cells (DCs) [Fainaru et al., 2004], natural killer cells [Ohno et al., 2008], B cells [Watanabe et al., 2010], and proprioceptive dorsal root ganglion neurons [Inoue et al., 2002; Levanon et al., 2002].

Immunoglobulin A (IgA) is the most abundantly produced Ig in vivo. In contrast to IgG, which plays a key role in systemic immune reactions through secretion into the blood, IgA is predominantly secreted into the gastrointestinal tract. In addition to the protection against mucosal pathogenic microorganisms, neutralization of toxins, and protection from epithelial penetration of microorganisms, IgA controls the size and species of the bacterial flora in the intestine [Cerutti and Rescigno, 2008; Macpherson et al., 2008; Mora and von Andrian, 2009; Stavnezer and Kang, 2009; Fagarasan et al., 2010]. Among the various factors, TGF-β1 plays a special role in IgA class switch recombination (CSR) because TGF-β1 is required for IgA switch induction of splenic B cells in vitro [Sonoda et al., 1989]; it was also reported that TGF-β1-deficient and B cell-specific TGF-β1 receptor II-deficient mice have low levels of IgA [van Ginkel et al., 1999; Cazac and Roes, 2000]. Recent findings indicate that Runx proteins play essential roles in this signaling pathway [Shi and Stavnezer, 1998; Hanai et al., 1999; Pardali et al., 2000; Zhang and Derynck, 2000; Ito and Miyazono, 2003; Miyazono et al., 2004; Javed et al., 2008].

CSR REGULATION

Humoral immunity is dependent on the expression of antibodies that are specific for foreign antigens and that possess specialized effector functions. To generate diverse antigen receptors, variable (V), diversity (D), and joining (J) gene segments are assembled through a process known as VDJ recombination during early B cell development. After migration to secondary lymphoid organs, antigen-stimulated mature B cells replace their Cμ constant region gene with other constant region isotypes through CSR. Therefore, CSR is required for the expression of antibodies that have the same antigen specificity but a different effector function. This process is mediated by an intrachromosomal recombinational event between the switch (S) region of the Cμ region and one of the downstream S regions. The target specificities of CSR are determined by cytokines through the control of germ line transcription (GLT) [Honjo et al., 2002; Chaudhuri and Alt, 2004; Ramiro and Nussenzweig, 2004; Sugai et al., 2005; Longerich et al., 2006; Stavnezer et al., 2008]. For example, interferon-γ induces GLT of γ2a, whereas TGF-β1 induces GLT of γ2b and α. On the other hand, interleukin-4 induces GLT of γ1 and ε. GLT initiates CSR by

*Correspondence to: Dr. Manabu Sugai, Translational Research Center, Kyoto University Hospital, 54 Shogoin-Kawahara-cho, Sakyo-ku, Kyoto 606-8507, Japan. E-mail: msugai@virus.kyoto-u.ac.jp

Received 16 November 2010; Accepted 17 November 2010 • DOI 10.1002/jcb.22971 • © 2010 Wiley-Liss, Inc.
Published online 6 December 2010 in Wiley Online Library (wileyonlinelibrary.com).

recruiting activation-induced cytidine deaminase (AID) to target loci [Nambu et al., 2003]. Recent studies indicated that stalled RNA polymerase II and Stg5 are required for AID recruitment to target loci [Pavri et al., 2010]. After deamination of the deoxycytidine at the transcribed S regions by AID, double-strand breaks generated by base excision repair or mismatch repair machineries are repaired by the nonhomologous end joining pathway [Honjo et al., 2002; Chaudhuri and Alt, 2004; Ramiro and Nussenzweig, 2004; Sugai et al., 2005; Longerich et al., 2006; Stavnezer et al., 2008] (Fig. 1).

SITES AND FACTORS FOR GENERATION OF IgA-PRODUCING CELLS

In germ-free mice, IgA production in the intestinal mucosa is severely affected; however, the IgA production normalizes within a few weeks following intestinal bacterial colonization. Thus, IgA production depends on bacterial stimulation in the intestine [Hooper and Macpherson, 2010]. Accordingly, skewed IgA CSR occurs in gut-associated lymphoid tissues (GALTs) called Peyer's patches, isolated lymphoid follicles, and the lamina propria (LP) of the intestine [Cerutti and Rescigno, 2008; Macpherson et al., 2008; Stavnezer and Kang, 2009; Fagarasan et al., 2010; Hooper and Macpherson, 2010]. However, the serum IgA level in germfree mice is maintained at approximately half the level maintained in normal mice, suggesting that serum IgA is partly produced in a manner independent of mucosal IgA.

In general, CSR requires two signals; one stimulates GLT of specific isotypes induced by several cytokines, and another is delivered by ligation of CD40 on B cells with the CD40 ligand (CD40L) on activated T cells. However, IgA production is not so abrogated in CD40- or CD40L-deficient mice and humans,

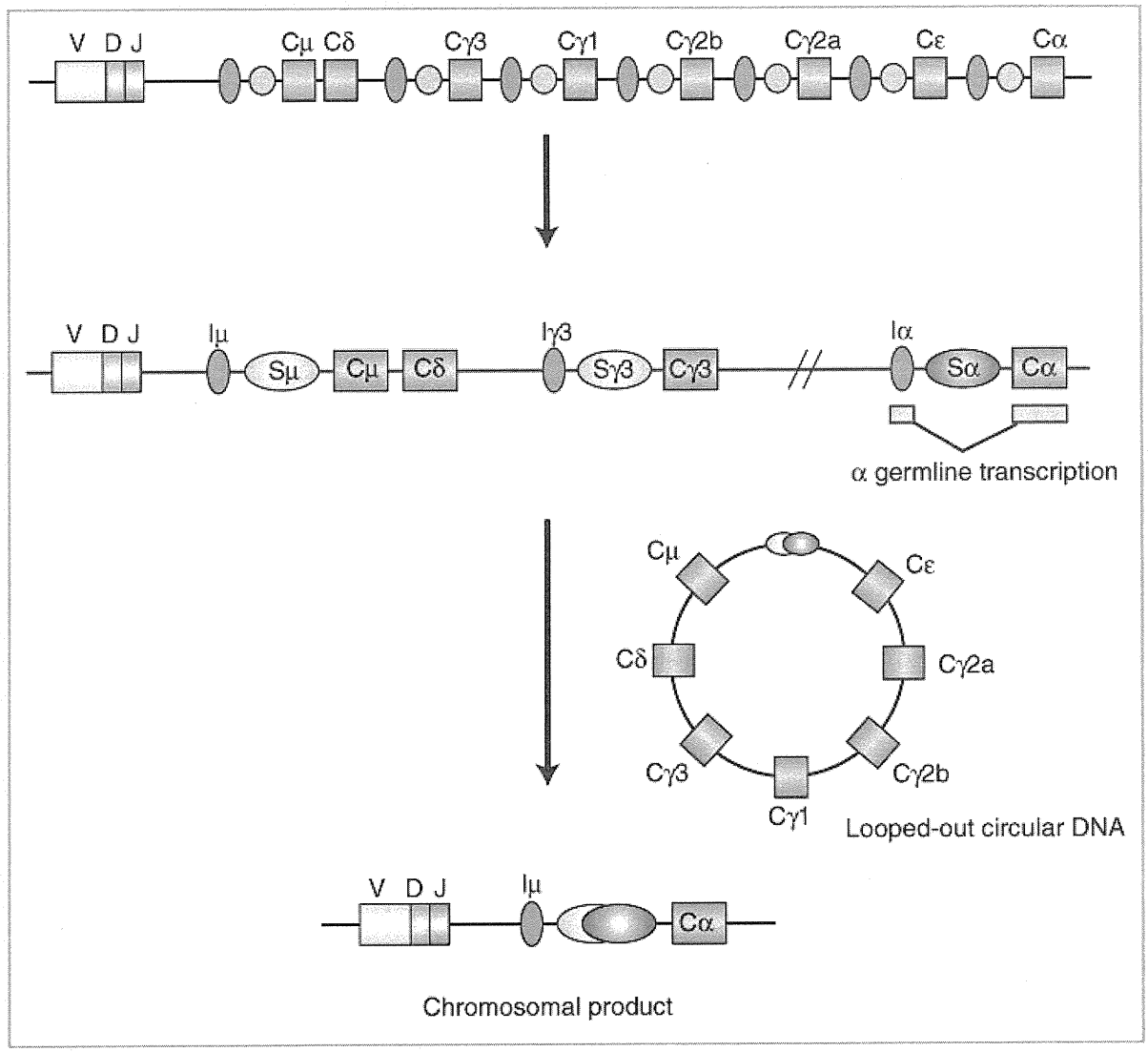

Fig. 1. Schematic representation of the murine heavy chain locus. The variable region of the immunoglobulin heavy chain gene is assembled from VH, DH, and JH gene segments by VDJ recombination. After completing VDJ recombination at heavy and light chain loci, B cells produce IgM antibody. Subsequently, secondary isotypes are produced by CSR, which exchanges the Cμ constant region gene for other downstream constant region genes. The CSR target is determined by cytokines through the induction of GLT at the target locus. For IgA CSR, TGF-β1 and RAs induce αGLT and promote IgA CSR.

indicating the existence of other costimulatory signals for IgA CSR. As expected, B cell-activating factor of tumor necrosis factor family (BAFF, also known as BLyS) and a proliferation-inducing ligand (APRIL) were identified as structurally and functionally related to CD40L and were found to stimulate CSR to IgG and IgA in vitro. B cells express three receptors for these cytokines, BAFF receptor (BAFF-R), transmembrane activator, and CAML interactor (TACI), and B cell maturation antigen (BCMA). BAFF interacts with all three receptors, whereas APRIL binds BCMA and TACI. Because BAFF- or BAFF-R-deficient mice display defects in B cell generation, IgA CSR cannot be estimated in these models. TACI mutations have been found in IgA-deficient and common variable immunodeficient individuals. In addition, TACI-deficient mice show low IgA levels [von Bulow et al., 2001]. One line of APRIL-deficient mice displayed IgA deficiency [Castigli et al., 2004], while another line that generated independently showed normal IgA levels [Varfolomeev et al., 2004]. The biological relevance of BAFF and APRIL signaling in IgA CSR was thus estimated. Recently, it was reported that a DC subset from small intestinal LP and GALT produces BAFF and APRIL via Toll-like receptor (TLR) signaling [Tezuka et al., 2007] (Fig. 2), the family of which comprises various pattern recognition receptor families that are required for sensing microorganisms by recognizing several molecules expressed by these microorganisms. In addition, it was demonstrated that human colon epithelial cells express BAFF and APRIL during

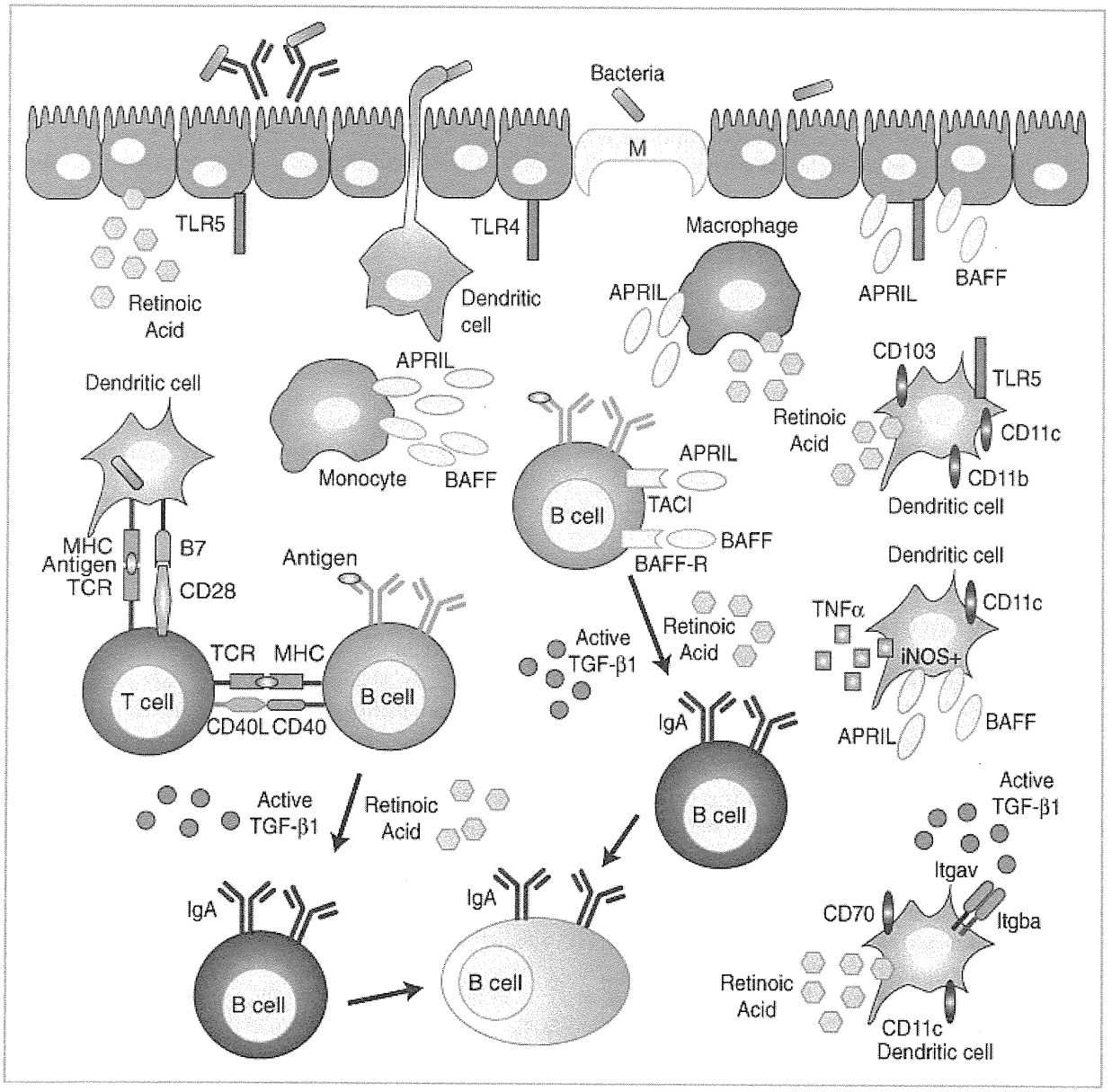

Fig. 2. IgA production in the intestine. IgA CSR requires T cell help (CD40L) or BAFF/APRIL signaling. In addition to these signals, all-trans retinoic acids and TGF-β1 are required for inducing αGLT. In the intestine, epithelial cells, DCs, macrophages, and monocytes produce APRIL and BAFF. In addition, many cell types produce RA as shown here. Recent studies indicated that there are various DC subsets within the intestine; known surface markers and their cytokine-producing properties are also shown.

stimulation with TLR (Fig. 2). These activities are believed to contribute to local switching to IgA in the colon.

The involvement of retinoic acids (RAs) in IgA production was demonstrated previously using vitamin A-deficient mice and rats. In vitamin A-deficient mice, reduced numbers of IgA-producing cells were observed in LP of the small intestine; the level of IgA in the serum, however, was not affected [Mora et al., 2006]. Thus, the effect of RA on IgA production is not systemic but is specific to the intestine. Recent studies further indicated that DCs from GALT or LP, but not from the spleen, have the ability to enhance IgA CSR partly by producing RA via the oxidation of RA precursors [Mora et al., 2006; Uematsu et al., 2008] (Fig. 2). Several reports further noted that intestinal epithelial cells and intestinal LP macrophages also express retinal dehydrogenases and secrete RA (Fig. 2). Analysis of mice deficient in the inducible form of nitric oxide synthase (iNOS) showed that IgA CSR in vivo is dependent on this enzyme. iNOS is expressed by DCs from LP and GALT but not from the spleen, and this expression of iNOS depends on TLR signaling (Fig. 2). NO produced by iNOS appears to be important for the normal expression of TGF-β1 receptor II, Smad3, and Runx3 in activated B cells, as well as for the production of BAFF and APRIL by DCs [Tezuka et al., 2007].

It is also well known that GALT and LP are rich in TGF-β1. In addition, subsets of LPDCs and LP stromal cells (LSCs) promote IgA CSR partly through TGF-β1 secretion. Moreover, mucosal DCs express the integrins αvβ6 and αvβ8, which activate latent TGF-β1 in vivo [Atarashi et al., 2008] (Fig. 2). These findings further support the hypothesis that GALTs are rich in IgA-inducing factors, and thus skewed IgA CSR takes place in the intestine. In summary, various intestinal cells have sensing systems for bacterial invasion, one of which is TLR, and these cells utilize the sensing signals to create optimal conditions for IgA CSR promotion.

RUNX FUNCTIONS IN IgA PRODUCTION

As described above, various types of cells in the intestinal region contribute to the establishment of optimal conditions for skewed IgA CSR. Because Runx proteins are expressed in intestinal epithelial cells, DCs, macrophages, T cells, and B cells, the functions of Runx may include the regulation of IgA production in vivo [Mora and von Andrian, 2009]. Among the three Runx proteins, special attention has been paid to Runx3, as loss of this protein is associated with defects in DC function and development of colitis and asthma-like features [Brenner et al., 2004; Fainaru et al., 2004]. Runx3-deficient mice have a defect in DC function in response to TGF-β1, which is not believed to be directly related to its function in IgA production. On the other hand, accumulating evidence indicates that Runx3 is a positive regulator for CD103 expression in various cell types [Grueter et al., 2005]. Furthermore, it was shown that mucosal CD103+ DCs can induce regulatory T cells via TGF-β1 and RA-dependent mechanisms [Coombes et al., 2007]; both these factors are also required for IgA CSR (Fig. 2). Accordingly, it is believed that Runx3 should work as a positive regulator for IgA CSR acting within DCs. However, to elucidate its role, further and more extensive investigations are required.

Several studies revealed that Runx transcription factors act in concert with Smad proteins in their response to the signals of the TGF-βfamily. Runx and Smad proteins interact with each other and can enhance transcription synergistically, as demonstrated in reporter assays using the promoter of αGLT [Shi and Stavnezer, 1998; Hanai et al., 1999; Pardali et al., 2000; Zhang and Derynck, 2000; Javed et al., 2008]. Expression analysis of various Runx proteins in I.29, CH12, and splenic B cells under IgA-inducing conditions suggests that Runx3 is responsible for IgA CSR [Shi and Stavnezer, 1998]. Therefore, Runx3 is believed to function as an activator of IgA CSR in B cells. In this regard, Groner et al. demonstrated that Runx3-deficient B cells exhibited impaired IgA CSR in vitro, whereas the IgA levels in bronchoalveolar lavage from Runx3-dificient mice were increased significantly. Such discrepancies can be attributed partly to the difficulty in investigating IgA CSR in vitro. At the time of the study by Groner et al., the efficiency of the in vitro IgA CSR system was extremely low. In our recent study, we examined the effect of Runx3-deficiency in IgA CSR in a different genetic background using the same experimental setting and confirmed the results from Groner's study; we found that Runx3 exhibits some positive role in IgA CSR. However, defects in IgA CSR of Runx3-deficient B cells cannot be observed always, which indicates that various unknown factors may affect the results. Because all three Runx proteins are expressed in B cells and Runx1 is required for hematopoietic stem cell generation, we examined the effects of Runx2 and Runx3 on IgA CSR. Furthermore, Runx2- and Runx3-deficient mice died within a short period after birth; therefore, we generated Runx2/3-deficient lymphocytes in $RAG2^{-/-}$ mice by infusing Runx2/3-deficient fetal liver cells. As expected, IgA production was almost completely blocked in the $RAG2^{-/-}$ mice having Runx2/3-deficient lymphocytes [Watanabe et al., 2010].

To determine the Runx protein signals involved in IgA CSR, we established an efficient IgA CSR system using only soluble factors and found that RA and TGF-β1 act in synergy to induce IgA CSR. In this in vitro IgA switching system, APRIL played a special role. The addition of APRIL, but not BAFF, to the culture system enhanced the efficiency of IgA CSR significantly. We further determined the effect of APRIL on αGLT and found that the enhancement was not significant. Moreover, APRIL may have promoted cell survival in this specialized culture system. Therefore, we propose that APRIL and BAFF function as B cell survival factors in various IgA switch-inducing conditions in vivo, in addition to their known functions in inducing αGLT. Using this system, we found that Runx proteins are required not only for TGF-β1-dependent IgA CSR but also for RA-dependent IgA CSR. The existence of both pathways in IgA CSR is supported by observations where serum IgA levels in $RAG2^{-/-}$ mice with Runx2/3-deficient lymphocytes were found to be lower than the serum IgA levels in TGF-β1-deficient mice.

In Runx2/3-deficient B cells, IgA CSR by TGF-β1 is completely blocked. This indicates that TGF-β1-Smad signaling pathways work only in the presence of Runx proteins at the αGL promoter. In addition, Runx binding to Smad proteins and TAZ are not required for induction of αGLT and consequent IgA CSR. Therefore, Runx proteins function as synergistic coregulators of αGLT or provide accessible chromatin structures to Smad proteins, independent of their interaction.

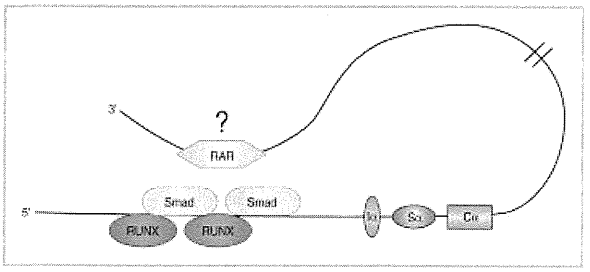

Fig. 3. Regulation of α germline promoter αGL promoter contains Runx and Smad binding sites but not RARE.

The involvement of Runx proteins in RA-dependent IgA CSR was confirmed using Runx2/3-deficient B cells. However, we could not determine the exact retinoic acid receptor response element (RARE) within the αGL promoter. Elucidating the mechanism of action of RAR and Runx proteins in the induction of αGLT is the next important issue. Currently, we are investigating the genuine RARE within the 3' enhancer of the heavy chain locus as well as examining the physical interaction between Runx and RAR proteins (Fig. 3).

In conclusion, we report that Runx proteins play pivotal roles in establishing good relationships between various commensal bacteria and provide a healthy intestinal environment by regulating the action of various cell types, including epithelial cells, DCs, T cells, and B cells in the intestine. Increased knowledge of the functions of Runx proteins in these cell types will facilitate the understanding of how Runx proteins work in general. This information is expected to contribute to understanding the functions of Runx proteins in tumorigenesis, cell differentiation, and other important biological issues.

ACKNOWLEDGMENTS

We thank our colleagues who have contributed to the study of IgA CSR and apologize for not including all references in this review because of space limitations. Published work from this laboratory was supported by Grants-in-Aid for Science Research on priority areas from the Ministry of Education, Culture, Sports, Science, and Technology of Japan.

REFERENCES

Atarashi K, Nishimura J, Shima T, Umesaki Y, Yamamoto M, Onoue M, Yagita H, Ishii N, Evans R, Honda K, Takeda K. 2008. ATP drives lamina propria T(H)17 cell differentiation. Nature 455:808–812.

Brenner O, Levanon D, Negreanu V, Golubkov O, Fainaru O, Woolf E, Groner Y. 2004. Loss of Runx3 function in leukocytes is associated with spontaneously developed colitis and gastric mucosal hyperplasia. Proc Natl Acad Sci U S A 101:16016–16021.

Castigli E, Scott S, Dedeoglu F, Bryce P, Jabara H, Bhan AK, Mizoguchi E, Geha RS. 2004. Impaired IgA class switching in APRIL-deficient mice. Proc Natl Acad Sci U S A 101:3903–3908.

Cazac BB, Roes J. 2000. TGF-beta receptor controls B cell responsiveness and induction of IgA in vivo. Immunity 13:443–451.

Cerutti A, Rescigno M. 2008. The biology of intestinal immunoglobulin A responses. Immunity 28:740–750.

Chaudhuri J, Alt FW. 2004. Class-switch recombination: interplay of transcription, DNA deamination and DNA repair. Nat Rev Immunol 4: 541–552.

Chen MJ, Yokomizo T, Zeigler BM, Dzierzak E, Speck NA. 2009. Runx1 is required for the endothelial to haematopoietic cell transition but not thereafter. Nature 457:887–891.

Coombes JL, Siddiqui KR, Arancibia-Carcamo CV, Hall J, Sun CM, Belkaid Y, Powrie F. 2007. A functionally specialized population of mucosal CD103+ DCs induces Foxp3+ regulatory T cells via a TGF-beta and retinoic acid-dependent mechanism. J Exp Med 204:1757–1764.

Fagarasan S, Kawamoto S, Kanagawa O, Suzuki K. 2010. Adaptive immune regulation in the gut: T cell-dependent and T cell-independent IgA synthesis. Annu Rev Immunol 28:243–273.

Fainaru O, Woolf E, Lotem J, Yarmus M, Brenner O, Goldenberg D, Negreanu V, Bernstein Y, Levanon D, Jung S, Groner Y. 2004. Runx3 regulates mouse TGF-beta-mediated dendritic cell function and its absence results in airway inflammation. Embo J 23:969–979.

Grueter B, Petter M, Egawa T, Laule-Kilian K, Aldrian CJ, Wuerch A, Ludwig Y, Fukuyama H, Wardemann H, Waldschuetz R, Moroy T, Taniuchi I, Steimle V, Littman DR, Ehlers M. 2005. Runx3 regulates integrin alpha E/CD103 and CD4 expression during development of CD4-/CD8+ T cells. J Immunol 175: 1694–1705.

Hanai J, Chen LF, Kanno T, Ohtani-Fujita N, Kim WY, Guo WH, Imamura T, Ishidou Y, Fukuchi M, Shi MJ, Stavnezer J, Kawabata M, Miyazono K, Ito Y. 1999. Interaction and functional cooperation of PEBP2/CBF with Smads. Synergistic induction of the immunoglobulin germline Calpha promoter. J Biol Chem 274:31577–31582.

Honjo T, Kinoshita K, Muramatsu M. 2002. Molecular mechanism of class switch recombination: linkage with somatic hypermutation. Annu Rev Immunol 20:165–196.

Hooper LV, Macpherson AJ. 2010. Immune adaptations that maintain homeostasis with the intestinal microbiota. Nat Rev Immunol 10:159–169.

Inoue K, Ozaki S, Shiga T, Ito K, Masuda T, Okado N, Iseda T, Kawaguchi S, Ogawa M, Bae SC, Yamashita N, Itohara S, Kudo N, Ito Y. 2002. Runx3 controls the axonal projection of proprioceptive dorsal root ganglion neurons. Nat Neurosci 5:946–954.

Ito Y, Miyazono K. 2003. RUNX transcription factors as key targets of TGF-beta superfamily signaling. Curr Opin Genet Dev 13:43–47.

Javed A, Bae JS, Afzal F, Gutierrez S, Pratap J, Zaidi SK, Lou Y, van Wijnen AJ, Stein JL, Stein GS, Lian JB. 2008. Structural coupling of Smad and Runx2 for execution of the BMP2 osteogenic signal. J Biol Chem 283: 8412–8422.

Kohu K, Sato T, Ohno S, Hayashi K, Uchino R, Abe N, Nakazato M, Yoshida N, Kikuchi T, Iwakura Y, Inoue Y, Watanabe T, Habu S, Satake M. 2005. Overexpression of the Runx3 transcription factor increases the proportion of mature thymocytes of the CD8 single-positive lineage. J Immunol 174: 2627–2636.

Komori T, Yagi H, Nomura S, Yamaguchi A, Sasaki K, Deguchi K, Shimizu Y, Bronson RT, Gao YH, Inada M, Sato M, Okamoto R, Kitamura Y, Yoshiki S, Kishimoto T. 1997. Targeted disruption of Cbfa1 results in a complete lack of bone formation owing to maturational arrest of osteoblasts. Cell 89: 755–764.

Levanon D, Bettoun D, Harris-Cerruti C, Woolf E, Negreanu V, Eilam R, Bernstein Y, Goldenberg D, Xiao C, Fliegauf M, Kremer E, Otto F, Brenner O, Lev-Tov A, Groner Y. 2002. The Runx3 transcription factor regulates development and survival of TrkC dorsal root ganglia neurons. Embo J 21:3454–3463.

Li QL, Ito K, Sakakura C, Fukamachi H, Inoue K, Chi XZ, Lee KY, Nomura S, Lee CW, Han SB, Kim HM, Kim WJ, Yamamoto H, Yamashita N, Yano T, Ikeda T, Itohara S, Inazawa J, Abe T, Hagiwara A, Yamagishi H, Ooe A, Kaneda A, Sugimura T, Ushijima T, Bae SC, Ito Y. 2002. Causal relationship between the loss of RUNX3 expression and gastric cancer. Cell 109:113–124.

Longerich S, Basu U, Alt F, Storb U. 2006. AID in somatic hypermutation and class switch recombination. Curr Opin Immunol 18:164–174.

Macpherson AJ, McCoy KD, Johansen FE, Brandtzaeg P. 2008. The immune geography of IgA induction and function. Mucosal Immunol 1:11–22.

Miyazono K, Maeda S, Imamura T. 2004. Coordinate regulation of cell growth and differentiation by TGF-beta superfamily and Runx proteins. Oncogene 23:4232–4237.

Mora JR, Iwata M, Eksteen B, Song SY, Junt T, Senman B, Otipoby KL, Yokota A, Takeuchi H, Ricciardi-Castagnoli P, Rajewsky K, Adams DH, von Andrian UH. 2006. Generation of gut-homing IgA-secreting B cells by intestinal dendritic cells. Science 314:1157–1160.

Mora JR, von Andrian UH. 2009. Role of retinoic acid in the imprinting of gut-homing IgA-secreting cells. Semin Immunol 21:28–35.

Nambu Y, Sugai M, Gonda H, Lee CG, Katakai T, Agata Y, Yokota Y, Shimizu A. 2003. Transcription-coupled events associating with immunoglobulin switch region chromatin. Science 302:2137–2140.

Ohno S, Sato T, Kohu K, Takeda K, Okumura K, Satake M, Habu S. 2008. Runx proteins are involved in regulation of CD122, Ly49 family and IFN-gamma expression during NK cell differentiation. Int Immunol 20:71–79.

Okuda T, van Deursen J, Hiebert SW, Grosveld G, Downing JR. 1996. AML1, the target of multiple chromosomal translocations in human leukemia, is essential for normal fetal liver hematopoiesis. Cell 84:321–330.

Osato M. 2004. Point mutations in the RUNX1/AML1 gene: another actor in RUNX leukemia. Oncogene 23:4284–4296.

Otto F, Thornell AP, Crompton T, Denzel A, Gilmour KC, Rosewell IR, Stamp GW, Beddington RS, Mundlos S, Olsen BR, Selby PB, Owen MJ. 1997. Cbfa1, a candidate gene for cleidocranial dysplasia syndrome, is essential for osteoblast differentiation and bone development. Cell 89:765–771.

Pardali E, Xie XQ, Tsapogas P, Itoh S, Arvanitidis K, Heldin CH, ten Dijke P, Grundstrom T, Sideras P. 2000. Smad and AML proteins synergistically confer transforming growth factor beta1 responsiveness to human germ-line IgA genes. J Biol Chem 275:3552–3560.

Pavri R, Gazumyan A, Jankovic M, Di Virgilio M, Klein I, Ansarah-Sobrinho C, Resch W, Yamane A, San-Martin BR, Barreto V, Nieland TJ, Root DE, Casellas R, Nussenzweig MC. 2010. Activation-induced cytidine deaminase targets DNA at sites of RNA polymerase II stalling by interaction with Spt5. Cell 143:122–133.

Ramiro AR, Nussenzweig MC. 2004. Immunology: aid for AID. Nature 430:980–981.

Sato T, Ohno S, Hayashi T, Sato C, Kohu K, Satake M, Habu S. 2005. Dual functions of Runx proteins for reactivating CD8 and silencing CD4 at the commitment process into CD8 thymocytes. Immunity 22:317–328.

Shi MJ, Stavnezer J. 1998. CBF alpha3 (AML2) is induced by TGF-beta1 to bind and activate the mouse germline Ig alpha promoter. J Immunol 161: 6751–6760.

Sonoda E, Matsumoto R, Hitoshi Y, Ishii T, Sugimoto M, Araki S, Tominaga A, Yamaguchi N, Takatsu K. 1989. Transforming growth factor beta induces IgA production and acts additively with interleukin 5 for IgA production. J Exp Med 170:1415–1420.

Stavnezer J, Guikema JE, Schrader CE. 2008. Mechanism and regulation of class switch recombination. Annu Rev Immunol 26:261–292.

Stavnezer J, Kang J. 2009. The surprising discovery that TGF beta specifically induces the IgA class switch. J Immunol 182:5–7.

Sugai M, Gonda H, Nambu Y, Yokota Y, Shimizu A. 2005. Accessibility control of recombination at immunoglobulin locus. Curr Immunol Rev 1:69–79.

Taniuchi I, Osato M, Egawa T, Sunshine MJ, Bae SC, Komori T, Ito Y, Littman DR. 2002. Differential requirements for Runx proteins in CD4 repression and epigenetic silencing during T lymphocyte development. Cell 111:621–633.

Tezuka H, Abe Y, Iwata M, Takeuchi H, Ishikawa H, Matsushita M, Shiohara T, Akira S, Ohteki T. 2007. Regulation of IgA production by naturally occurring TNF/iNOS-producing dendritic cells. Nature 448:929–933.

Uematsu S, Fujimoto K, Jang MH, Yang BG, Jung YJ, Nishiyama M, Sato S, Tsujimura T, Yamamoto M, Yokota Y, Kiyono H, Miyasaka M, Ishii KJ, Akira S. 2008. Regulation of humoral and cellular gut immunity by lamina propria dendritic cells expressing Toll-like receptor 5. Nat Immunol 9:769–776.

van Ginkel FW, Wahl SM, Kearney JF, Kweon MN, Fujihashi K, Burrows PD, Kiyono H, McGhee JR. 1999. Partial IgA-deficiency with increased Th2-type cytokines in TGF-beta 1 knockout mice. J Immunol 163:1951–1957.

Varfolomeev E, Kischkel F, Martin F, Seshasayee D, Wang H, Lawrence D, Olsson C, Tom L, Erickson S, French D, Schow P, Grewal IS, Ashkenazi A. 2004. APRIL-deficient mice have normal immune system development. Mol Cell Biol 24:997–1006.

von Bulow GU, van Deursen JM, Bram RJ. 2001. Regulation of the T-independent humoral response by TACI. Immunity 14:573–582.

Wang Q, Stacy T, Binder M, Marin-Padilla M, Sharpe AH, Speck NA. 1996. Disruption of the Cbfa2 gene causes necrosis and hemorrhaging in the central nervous system and blocks definitive hematopoiesis. Proc Natl Acad Sci U S A 93:3444–3449.

Watanabe K, Sugai M, Nambu Y, Osato M, Hayashi T, Kawaguchi M, Komori T, Ito Y, Shimizu A. 2010. Requirement for Runx proteins in IgA class switching acting downstream of TGF-beta 1 and retinoic acid signaling. J Immunol 184:2785–2792.

Zhang Y, Derynck R. 2000. Transcriptional regulation of the transforming growth factor-beta-inducible mouse germ line Ig alpha constant region gene by functional cooperation of Smad, CREB, and AML family members. J Biol Chem 275:16979–16985.

Carcinogenesis vol.32 no.1 pp.110–119, 2011
doi:10.1093/carcin/bgq222
Advance Access publication October 25, 2010

Activation of AID by human T-cell leukemia virus Tax oncoprotein and the possible role of its constitutive expression in ATL genesis

Chie Ishikawa[1,2], Sawako Nakachi[1,3], Masachika Senba[4], Manabu Sugai[5] and Naoki Mori[1,6,*]

[1]Department of Microbiology and Oncology, Graduate School of Medicine, University of the Ryukyus, Nishihara, Okinawa 903-0215, Japan, [2]Transdisciplinary Research Organization for Subtropics and Island Studies, University of the Ryukyus, Nishihara, Okinawa 903-0213, Japan, [3]Department of Endocrinology, Metabolism and Hematology, Graduate School of Medicine, University of the Ryukyus, Nishihara, Okinawa 903-0215, Japan, [4]Department of Pathology, Institute of Tropical Medicine, Nagasaki University, Nagasaki 852-8523, Japan and [5]Department of Experimental Therapeutics, Translational Research Center, Kyoto University Hospital, Kyoto 606-8507, Japan

[6]Present address: Department of Internal Medicine, Omoromachi Medical Center, 1-3-1 Uenoya, Naha, Okinawa, Japan

*To whom correspondence should be addressed. Department of Internal Medicine, Omoromachi Medical Center, 1-3-1 Uenoya, Naha, Okinawa 900-0011, Japan. Tel: +81 98 867 2116; Fax: +81 98 861 2398; Email: naokimori50@gmail.com

Adult T-cell leukemia (ATL) is a T-cell malignancy associated with human T-cell leukemia virus type 1 (HTLV-1). Mutations of tumor suppressor genes have been described in ATL. Although Tax, a product of HTLV-1, is associated with cellular genetic aberrations, the mechanisms of such association are not fully clear. Activation-induced cytidine deaminase (AID) is involved in somatic DNA alterations of the immunoglobulin gene for amplification of immune diversity. However, inappropriate expression of AID acts as a genomic mutator that contributes to tumorigenesis. To gain insight into the molecular mechanism underlying the emergence of somatic mutations in various genes during leukemogenesis, we examined the expression of AID. HTLV-1-infected T-cell lines and ATL cells expressed high levels of AID compared with uninfected T-cell lines and normal peripheral blood mononuclear cells (PBMCs). Immunohistochemistry showed AID-positive ATL cells in lymph nodes and skin lesions. Infection of a human T-cell line and normal PBMCs with HTLV-1 induced AID expression. Tax transcriptionally activated *AID* gene through both the nuclear factor-kappaB subunit p50 and cyclic adenosine 3′,5′-monophosphate response element-binding protein signaling pathways. p50, which lacks a transactivation domain, interacted with the transcriptional coactivator Bcl-3 in HTLV-1-infected T cells. Thus, activation of p50/Bcl-3 complexes in T cells in response to Tax might explain the constitutive expression of AID in HTLV-1-infected T cells. The constitutive expression of AID in ATL cells can be speculated to result from mutations induced by the Tax-activated AID and/or other Tax-associated mutagenic mechanisms during the pre-leukemic stage, which cause functional modification within the AID promoter or in any of its cellular regulatory activator proteins.

Introduction

Adult T-cell leukemia (ATL) is a highly aggressive malignancy of mature CD4+ T cells etiologically caused by human T-cell leukemia virus type 1 (HTLV-1) (1). ATL develops after a long period of latency, usually 40–60 years. The vast majority of infected persons remain clinically asymptomatic, whereas only 2–5% develop neoplasia. After infection of the T cells, ATL is thought to develop after a multitude of events including both genetic and epigenetic changes in the cell over time (2). Despite intensive studies on HTLV-1, the pathogenic mechanism(s) involved leukemogenesis remain not fully understood. However, the viral Tax protein is widely regarded as a key factor in this mechanism because of its capacity to stimulate or repress the synthesis or function of many regulatory factors involved in a wide range of normal and pathogenic cellular processes (3). By constitutive induction of regulatory factors involved in activation of T-cell replication, Tax protein can set infected T cells into a continuous uncontrolled replication. Tax affects both the fidelity of chromosomal segregation (aneuploidogenic) (4) and the mismatch repair (clastogenic) (5) functions. Mechanistically, Tax has been shown to abrogate the mitotic checkpoint function (3) and lead to miscounted chromosomes in HTLV-1-transformed T cells (6). Tax has also been shown to interfere with most DNA repair mechanisms, thus further intensifying the genome instability of these cells (7). Usually, cells that suffer from mitotic checkpoint dysfunction, or cannot repair damage imposed on their DNA, enter into cell-cycle arrest or apoptosis. In contrast, HTLV-1-infected T cells are protected by Tax from both these responses (7). Based on these pleiotropic activities, Tax acts as a potent oncoprotein capable of transforming cultured animal cells, inducing tumors in transgenic mice and immortalizing or transforming human primary T cells (7). Thus, the oncogenic potency of Tax is thought to initiate the leukemic process leading to ATL (7).

It is widely recognized that mutations of oncogenes, tumor suppressor genes and genomic stability genes play pivotal roles in carcinogenesis (8). Despite remarkable progress in our knowledge of the molecular mechanisms of individual cancer-related genes, surprisingly little is known about the fundamental aspects of when and how mutations are introduced into what kind of cell populations.

To address this problem, a new mechanism of mutagenesis in cancer development has been proposed recently (9,10). It is hypothesized that at least certain cancer-related mutations are introduced by activation-induced cytidine deaminase (AID), an enzyme expressed in activated B lymphocytes, and is required for somatic hypermutation and class-switch recombination of antibody genes (11). The hypothesis is based on the following observations: (i) AID can induce mutations in non-B cells (12), (ii) AID transgenic mice develop various tumors, including T-cell lymphoma and lung microadenoma (13) and (iii) AID can be induced in human hepatic and gastric epithelial cells when challenged with pathogens such as hepatitis C virus and *Helicobacter pylori* (14,15). On the basis of this evidence, AID is a potential candidate mutagen in human cancers.

Based on the above background, we hypothesized that aberrant expression of AID in HTLV-1-infected T cells plays a role in the enhanced genetic susceptibility to mutagenesis during leukemogenesis. In the present study, we examined the expression of AID in various T-cell lines and clinical samples from patients with ATL. The purpose of the study was to determine whether Tax induces the expression of AID and the molecular mechanism by which AID is induced by Tax. Our findings may provide a molecular explanation for the clastogenic effect of Tax.

Abbreviations: AID, activation-induced cytidine deaminase; ATL, adult T-cell leukemia; B-ALL, B-lineage acute lymphoblastic leukemia; CRE, cyclic adenosine 3′,5′-monophosphateresponse element; CREB, CRE-binding protein; EMSA, electrophoretic mobility shift assay; FBS, fetal bovine serum; HTLV-1, human T-cell leukemia virus type 1; IgG, immunoglobulin G; IKK, IκB kinase; IL, interleukin; MMC, mitomycin C; NF-κB, nuclear factor-kappaB; PBMC, peripheral blood mononuclear cell; PBS, phosphate-buffered saline; PCR, polymerase chain reaction; RT, reverse transcription; siRNA, small interfering RNA; T-ALL, T-lineage ALL.

Materials and methods

Cells

HTLV-1-infected T-cell lines MT-2 (16), MT-4 (17), C5/MJ (18), TL-OmI (19) and ED-40515(-) (20), HTLV-1-uninfected T-cell lines Jurkat, MOLT-4 and CCRF–CEM and Burkitt lymphoma cell line Ramos were cultured in RPMI 1640 medium supplemented with 10% heat-inactivated fetal bovine serum

(FBS; Biological Industries, Kibbutz Beit Haemek, Israel), 50 U/ml of penicillin and 50 μg/ml of streptomycin. MT-2, MT-4 and C5/MJ are HTLV-1-transformed T-cell lines and constitutively express viral genes including *Tax*. TL-OmI and ED-40515(-) are T-cell lines of leukemic cell origin that were established from patients with ATL and do not express viral genes. JPX-9 is a subline of Jurkat that expresses Tax under the control of the *metallothionein* gene promoter (21). Peripheral blood mononuclear cells (PBMCs) were isolated from 6 healthy volunteers, 20 patients with acute-type ATL, 1 patient with B-lineage acute lymphoblastic leukemia (B-ALL) and 2 patients with T-lineage acute lymphoblastic leukemia (T-ALL) using Ficoll–Paque density gradient centrifugation (GE Healthcare Biosciences, Uppsala, Sweden). Bone marrow samples from five patients with B-ALL were also obtained. For the usage of activated T cells, PBMCs were stimulated with 10 μg/ml phytohemagglutinin for 72 h. All samples were collected at the time of admission to hospital before the patients started chemotherapy. The diagnosis of ATL was based on clinical features, hematologic findings and the presence of anti-HTLV-1 antibodies in the sera. Monoclonal HTLV-1 provirus integration into the DNA of leukemic cells was confirmed by Southern blot hybridization in all patients (data not shown). This study was approved by the Institutional Review Board of the University of the Ryukyus. Informed consent was obtained from all blood and tissue donors in accordance with the Declaration of Helsinki.

Reagents

N-acetyl-L-leucyl-L-leucyl-L-norleucinal and Bay 11-7082 were purchased from Sigma–Aldrich (St Louis, MO) and Calbiochem (La Jolla, CA), respectively. Human recombinant p50 was obtained from Promega (Madison, WI).

Reverse transcription–polymerase chain reaction

Total RNA was extracted with Trizol (Invitrogen, Carlsbad, CA) according to the protocol provided by the manufacturer. First-strand complementary DNA was synthesized from 1 μg total cellular RNA using a RNA-polymerase chain reaction (PCR) kit (Takara Bio, Otsu, Japan) with random primers. The sequences of the primers were described previously (14,22–26). The p65 primer pairs were as follows: p65 sense, 5′-GCGGCCAAGCTTAAGATCTGCC-GAGTAAAC-3′ and antisense, 5′-GCGTGCTCTAGAGAACACAATGGC-CACTTGCCG-3′ The setting for semiquantitative reverse transcription (RT)–PCR for each gene was as follows: 25 cycles for p50/p100; 30 cycles for p65, Bcl-3 and Tax; 35 cycles for AID and apolipoprotein B messenger RNA-editing enzyme, catalytic polypeptide-like 3 (APOBEC3)G and 28 cycles for β-actin. The PCR products were fractionated on 2% agarose gels and visualized by ethidium bromide staining. The obtained bands of amplified DNA were quantified using AlphaEase FC software (Alpha Innotech Corporation, San Leando, CA). Data were normalized to β-actin loading controls.

Western blot analysis

Cells were lysed and equal amounts of protein (20 μg) were subjected to electrophoresis on sodium dodecyl sulfate–polyacrylamide gels, followed by transfer to a polyvinylidene difluoride membrane and sequential probing with rabbit monoclonal antibody to AID (Cell Signaling Technology, Beverly, MA), rabbit polyclonal antibody to Bcl-3 (Santa Cruz Biotechnology, Santa Cruz, CA) and mouse monoclonal antibodies to actin (NeoMarkers, Fremont, CA) and Tax, Lt-4 (27). The bands were visualized with an enhanced chemiluminescence kit (Amersham Biosciences, Piscataway, NJ).

Immunohistochemical analysis

Biopsy samples were taken from the lesional skin of 10 patients with ATL and lymph nodes of 6 patients with ATL. AID immunohistochemistry was performed using a mouse anti-AID monoclonal antibody (Zymed Laboratories, South San Francisco, CA) after pretreatment of the deparaffinized tissue sections with ready-to-use proteinase K (Dako, Carpinteria, CA). The sections were counterstained with methyl green, hydrated in ethanol and cleaned in xylene and mounted. The stained cells were examined under a light microscope (Axioskop 2plus; Zeiss, Jena, Germany) with an Achroplan ×40/0.65 lens (Zeiss). Images were acquired with an AxioCam MRC camera and AxioVision 3.1 software (Zeiss).

Immunofluorescence staining

Cells were fixed with 4% paraformaldehyde for 20 min at 37°C. Fixed cells were washed with phosphate-buffered saline (PBS) containing 7% of FBS twice and permeabilized with PBS containing 0.1% Triton X-100 for 10 min at room temperature. The cells were washed with PBS containing 7% of FBS once and resuspended in PBS/7% FBS containing rabbit polyclonal antibody to Bcl-3 (Santa Cruz Biotechnology) and mouse monoclonal antibody to p50 (Santa Cruz Biotechnology) for 20 min at room temperature. The cells were washed with PBS/7% FBS twice and resuspended in PBS/7% FBS containing Alexa Fluor 488-labeled goat anti-mouse immunoglobulin G (IgG) and Alexa Fluor 546-labeled goat anti-rabbit IgG (Invitrogen) for 20 min at room temperature. The nuclei were stained with Hoechst 33342 (Wako Pure Chemical Industries, Osaka, Japan). Finally, the cells were washed with PBS twice and observed under a Leica DMI6000 microscope (Leica Microsystems, Wetzlar, Germany). Mounted coverslips were imaged through a ×63 oil immersion lens (NA1.4) on a Leica TCS SP5 confocal system.

HTLV-1 infection by cocultivation

HTLV-1-infected MT-2 cells were pretreated with 200 μg/ml of mitomycin C (MMC) for 60 min at 37°C, pipetted vigorously and washed three times with PBS. PBMCs from healthy donors (5×10^6 per well) and MMC-treated MT-2 cells (5×10^6 per well) were cocultured in a 24-well plate in the presence of 10 ng/ml of interleukin (IL)-2. The culture medium was half-changed with fresh medium supplemented with IL-2 every 3 days. TY8-3/MT-2 was established from the IL-2-dependent human T-cell line TY8-3 cocultured with MMC-treated MT-2 cells and was capable of growth completely independent of IL-2 (28).

Transfection and luciferase assay

Various expression vectors for Tax (pβMT-2 Tax) and its mutants (Tax M22 and Tax 703) were described previously (29). Tax M22 has an amino acid substitution at codons 130 and 131 from Thr–Leu to Ser–Ala. Tax 703 has an amino acid substitution at codons 319 and 320 from Leu–Leu to Arg–Ser, which is equivalent to mutant M47. Tax M22 effectively activates cyclic adenosine 3′,5′-monophosphate response element (CRE), which mediates the Tax-dependent activation of the HTLV-1 long terminal repeat but not the nuclear factor-kappaB (NF-κB) element. In contrast, Tax 703 activates the NF-κB element but does not affect CRE. The expression vectors for p65 and p50 were also used. The IκBαΔN- and IκBβΔN-dominant-negative mutants are IκBα and IκBβ deletion mutants lacking the N-terminal 36 and 23 amino acids, respectively (30,31). The dominant-negative mutants of IκB kinase (IKK)α, IKKα (K44M), IKKβ, IKKβ (K44A), IKKγ, IKKγ (1-305) and NF-κB-inducing kinase, NF-κB-inducing kinase (KK429/430AA) have been described previously (32,33). The dominant-negative mutants of cyclic adenosine 3′,5′-monophosphate response element-binding protein (CREB), pCMV-KCREB and pCMV-CREB133, were purchased from Clontech Laboratories (Mountain View, CA). Several luciferase expression constructs containing the AID promoter fragment into a pGL3 basic vector were described previously (34). The 0.9PΔκB construct was constructed by deletion of the NF-κB site of 0.9P (900 bp 5′ fragment only). Jurkat cells were transfected with the appropriate reporter and effector plasmids by electroporation. After 48 h, luciferase assays were performed with the dual luciferase assay system (Promega). Luciferase activities were normalized relative to the *Renilla* luciferase activity from phRL-TK.

Small interfering RNA

To repress p50 and p65, predesigned double-stranded small interfering RNAs (siRNAs; ON-TARGET plus SMART pool; Dharmacon, Lafayette, CO) were used. A siCONTROL non-targeting siRNA pool (Dharmacon) was used as a negative control. All siRNA transfections were performed using a MicroPorator MP-100 (Digital Bio Technology, Seoul, Korea), pulsed twice at 1100 V for 30 ms.

Preparation of nuclear extracts and electrophoretic mobility shift assay

Nuclear proteins were extracted and transcription factors bound to specific DNA sequences were examined by electrophoretic mobility shift assay (EMSA) as described previously (35). The top strand sequence of the oligonucleotide probe or competitors are as follows: for the NF-κB element of the *AID* gene, 5′-GATCGTCGTGGGGGAGGAGCCCACAAGA-3′; for the NF-κB element of the *IL-2 receptor α chain* gene, 5′-GATCCGGCAGGG-GAATCTCCCTCTC-3′; for the NF-κB element of the *inducible nitric oxide synthase* gene, 5′-TCGATGCTAGGGGGATTTTCCCTCTCTCTG-3′ and for the AP-1 element of the *IL-8* gene, 5′-GATCGTGATGACTCAGGTT-3′. The above underlined sequences are the NF-κB and AP-1-binding sites, respectively. To identify the transcription factors in the DNA-protein complex shown by EMSA, we used antibodies for various NF-κB family proteins, including p50, p65, c-Rel, p52 and RelB (Santa Cruz Biotechnology).

Immunoprecipitation and immunoblotting

To examine protein–protein interaction in MT-2 cells, whole-cell lysates were prepared from cells using lysis buffer (50 mM Tris, pH 8.0, 100 mM NaCl, 1 mM ethylenediaminetetraacetic acid, 0.5% NP-40 and 1 mM phenylmethylsulfonyl fluoride). Whole-cell extract was incubated with 2 μg of antibodies specific for Bcl-3 and p50 or control rabbit IgG for 4 h at 4°C on a rotator. Following incubation with the antibodies, lysates were incubated with Protein G Sepharose 4 Fast Flow (GE Healthcare, Piscataway, NJ) for 16 h at 4°C on a rotator. After washing the beads three times in ice-cold lysis buffer and once in wash buffer (50 mM Tris, pH 8.0), the beads were suspended in sample buffer (1% sodium dodecyl sulfate, 100 mM dithiothreitol and 50 mM Tris, pH

7.5). Before loading, the beads were boiled for 5 min, spun and the eluate was subjected to sodium dodecyl sulfate–polyacrylamide gels. Following transfer, blots were immunoblotted as in western analysis section. Mouse monoclonal antibody to p50 and rabbit polyclonal antibody to Bcl-3 (Santa Cruz Biotechnology) and rabbit polyclonal antibody to p50 (Cell Signaling Technology) were used for immunoprecipitation and western blot.

Results

AID expression in HTLV-1-infected T-cell lines and primary ATL cells

First, we examined the expression of Tax in various human T-cell lines (Figure 1A). Tax messenger RNA (mRNA) was highly expressed in HTLV-1-transformed T-cell lines (MT-2, MT-4 and C5/MJ) but not in ATL-derived T-cell lines, TL-Oml and ED-40515(-) cells. Tax protein was detected in all HTLV-1-transformed T-cell lines but not in any ATL-derived T-cell lines. We next examined the expression of AID at mRNA and protein levels in various human T-cell lines by RT–PCR and western blot analysis, respectively. As shown in Figure 1A, compared with uninfected T-cell lines, HTLV-1-transformed T-cell lines but not ATL-derived T-cell lines, expressed AID mRNA and protein (Figure 1A). APOBEC3 family, consisting of APOBEC3A-3H, consists of cellular proteins with cytidine deaminase activity that induces dC-to-dU mutations in minus-stranded DNA formed during RT to disable a broad range of retroviruses. APOBEC3G has been identified to potently inhibit the replication of human immunodeficiency virus type 1 (36). Expression of APOBEC3G mRNA was not associated with HTLV-1 infection (Figure 1A). Furthermore, we examined the mRNA expression of AID in primary ATL cells freshly isolated from acute-type patients and in PBMCs from normal subjects. Primary ATL cells from seven of nine patients expressed AID mRNA at significantly higher levels than normal PBMCs (Figure 1B). Tax protein was not expressed in all types of cells (data not shown). Phytohemagglutinin also induced AID mRNA expression (Figure 1C). To clarify whether AID expression is restricted to ATL cells, we examined AID mRNA expression in other lymphoid leukemia. However, no specific fragment could be amplified from B-ALL and T-ALL samples except for 1 B-ALL sample (Figure 1C). Immunohistochemical staining identified ATL cells positive for AID in the cytoplasm of all skin tissue (n = 10) and lymph node (n = 6) samples examined (Figure 1D), although the staining intensity varied from one specimen to another.

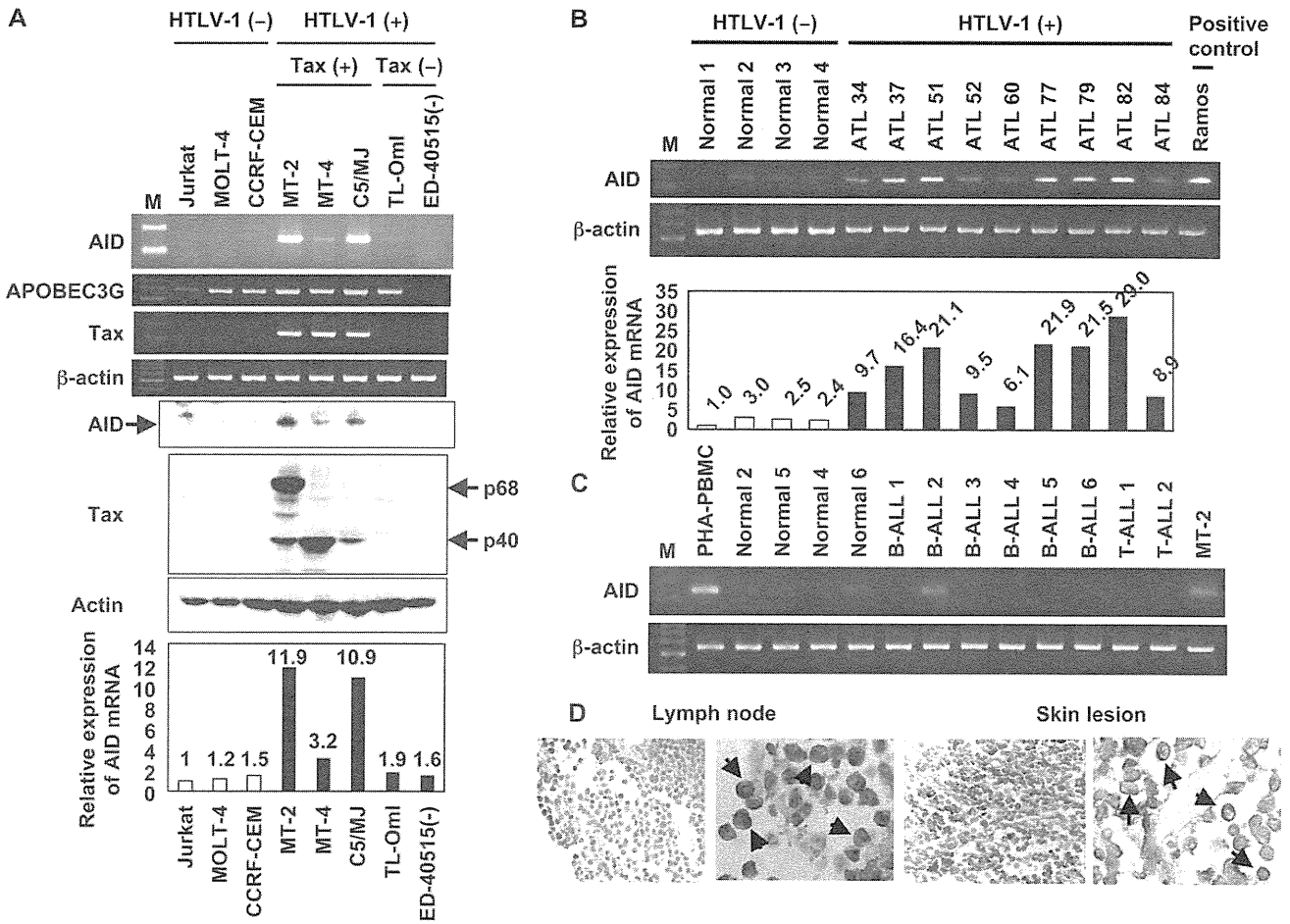

Fig. 1. AID is consistently expressed in HTLV-1-transformed T-cell lines and primary ATL cells. (**A**) Expression of AID, APOBEC3G and Tax in HTLV-1-infected T-cell lines. RT–PCR analysis was carried out for AID, APOBEC3G, Tax and β-actin (loading control). Western blot analysis was performed for AID, Tax and actin. Lt-4 monoclonal antibody detected a 40 kDa molecule (p40) in MT-4 and C5/MJ cells and p40 and p68 (a fusion between the envelope and the Tax-coding sequence) in MT-2 cells. Histograms indicate the relative density data of AID mRNA by densitometric analysis of the bands shown in the top panel normalized to β-actin mRNA (fourth panel). (**B**) RT–PCR analysis for AID expression in normal PBMCs and primary ATL cells. Normal PBMCs from healthy donors (n = 4) and freshly isolated primary ATL cells (>90% leukemic cells) from patients (n = 9) were examined as indicated. Histograms indicate the relative density data of AID mRNA obtained by densitometric analysis of the bands shown in the top panel normalized to β-actin mRNA (bottom). (**C**) RT–PCR analysis for AID expression in phytohemagglutinin-stimulated and -unstimulated PBMCs, B-ALL and T-ALL samples. Phytohemagglutinin–PBMC: normal PBMCs treated with phytohemagglutinin for 3 days. (**D**) Immunohistochemical staining of AID in ATL lymph nodes and skin lesions. Tissue sections from ATL lymph nodes (n = 6) and skin lesions (n = 10) were stained with anti-AID antibody. Tissue sections were counterstained using methyl green. Representative results from a single donor. The arrows indicate typical AID-positive tumor cells. Original magnification, ×400 and ×1200.

In lymph node, these AID-positive tumor cells were varying in size (medium and large) and showed severe nuclear irregularity. In skin tissue, these AID-positive tumor cells were varying in size (small to large) and showed mild to moderate nuclear irregularity.

AID expression during HTLV-1 infection

To examine whether HTLV-1 infection induces AID expression in PBMCs, we cocultured PBMCs and MMC-treated HTLV-1-infected MT-2 cells. At 7 days after cocultivation, PBMCs were harvested for assessment for expression of HTLV-1 viral gene by RT–PCR. PBMCs cocultured with MMC-treated MT-2 cells expressed Tax mRNA (Figure 2A). Furthermore, AID expression levels increased in these cells in conjunction with induction of HTLV-1 gene. Since MT-2 cells were pretreated extensively with MMC, no discernible MT-2 cells were seen. Trypan blue staining confirmed that no MT-2 cells were viable. This assured that no MMC-treated MT-2 cells persisted in the PBMCs culture at the time of RNA isolation. Previously, the possibility that gene amplification was due to the contamination from residual MT-2 cells was excluded (37,38). Furthermore, AID expression levels did not increase in PBMCs cocultured with MMC-treated Jurkat cells and the supernatants of MT-2 cells had no substantial effects on PBMCs (data not shown). These results suggest that infection of PBMCs with HTLV-1 induces expression of AID. Similarly, cocultivation of the human T-cell line TY8-3 with MMC-treated MT-2 cells upregulated AID expression (Figure 2B). Thus, infection with HTLV-1 induces the expression of AID in both PBMCs and a T cell line.

Tax-dependent expression of AID

Tax gene product is the primary viral transactivator protein that modulates the expression of both viral and cellular genes. To examine whether Tax induces AID expression, we used JPX-9 cells, a Jurkat subline that carries the *tax* gene under the control of the *metallothionein* gene promoter (21). Treatment of these cells with $CdCl_2$ rapidly induced the expression of Tax mRNA (Figure 2C) as well as AID mRNA expression. In contrast, this treatment did not show any effect in Jurkat cells (Figure 2C).

As shown in Figure 1B, the primary ATL cells isolated from not all patients expressed AID. We further examined the coexpression of AID and Tax in ATL cells cultured for 3 days. Although circulating ATL cells freshly isolated from patients (ATL 93 and 100) hardly expressed *Tax* mRNA, the expression level markedly increased after 24–72 h of culture. CpG methylation of the HTLV-1 long terminal repeat plays a critical role in repression of viral gene expression in latently infected cells (39). This increased *Tax* mRNA expression might be due to reactivation of viral gene expression. AID mRNA was also expressed in primary ATL cells after 24–72 h of culture in parallel with Tax mRNA (Figure 2D). Taken together, these results further support the view that Tax induces AID.

To test the effect of Tax on AID expression at the transcriptional level, we performed luciferase reporter assays in Jurkat cells using an AID promoter-luciferase reporter plasmid (34). Cotransfection of an expression vector for Tax strongly activated AID promoter dose and time dependently in Jurkat cells (Figure 3A), indicating that Tax directly activates the AID promoter.

To narrow down the transactivation-relevant signaling pathways, Tax mutants M22 and 703 (29) were cotransfected along with the AID promoter construct, followed by determination of luciferase activities. Tax M22, which can activate CREB but is defective in NF-κB activation, did not activate the AID promoter. Tax 703, which can activate NF-κB but not CREB, failed to activate the AID promoter. However, Tax mutants M22 and 703 together activated the AID promoter, although the levels were less than wild-type Tax (Figure 3B). These results suggest that Tax activates the AID promoter in NF-κB- and CREB-dependent manners.

We next examined whether Tax-mediated transactivation of *AID* gene expression involves signal transduction components in NF-κB

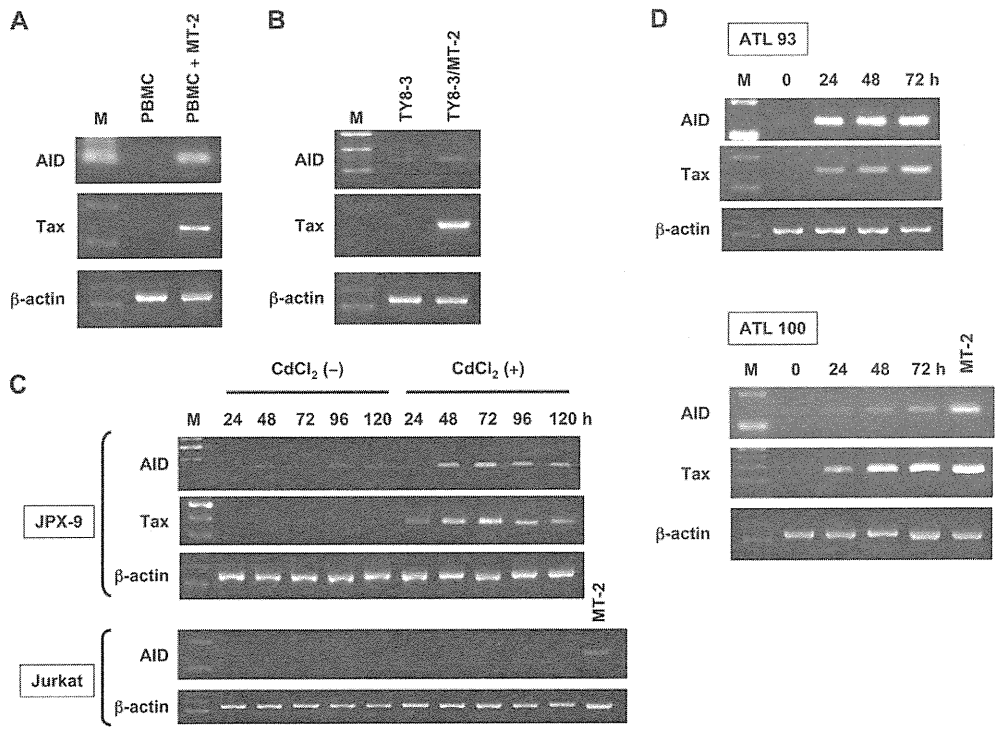

Fig. 2. HTLV-1 and Tax induce AID expression. (**A** and **B**) Expression of HTLV-1 Tax and AID during HTLV-1 infection of normal PBMCs and TY8-3. Normal PBMCs and TY8-3 were cocultured with or without MMC-treated MT-2 cells. After cocultivation, cells were harvested, and the expression of the indicated genes was analyzed by RT–PCR. β-actin mRNA was used as a control. (**C**) Induction of AID mRNA expression by Tax. JPX-9 and Jurkat cells were treated with or without 20 μM of $CdCl_2$ for the indicated time periods. RT–PCR was carried out for AID, Tax and β-actin (loading control). (**D**) RT–PCR analysis for AID and Tax expression in PBMC samples from patients with ATL (ATL 93 and 100) without or with 24–72 h of culture.

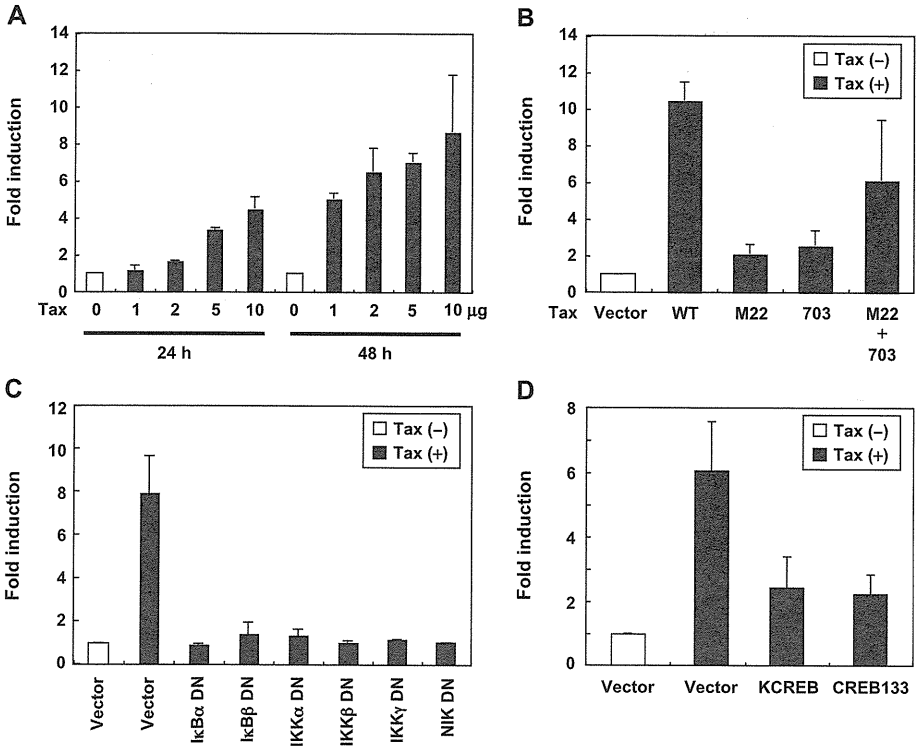

Fig. 3. Tax transactivates the AID promoter through both NF-κB and CREB pathways. (**A**) Effect of Tax overexpression on AID promoter. Jurkat cells were transfected with increasing amounts of expression plasmid for HTLV-1 Tax along with 0.9P (5 μg) using electroporation. Cells were harvested 24 or 48 h after transfection, and luciferase activity was measured with a luminometer. (**B**) Tax activates the AID promoter by NF-κB and CREB. Jurkat cells were transfected with 0.9P (5 μg) together with the expression vector for HTLV-1 Tax (Tax WT), Tax M22, Tax 703 or empty vector (10 μg) alone or the combination of Tax M22 and Tax 703. (**C**) Functional effects of IκBα, IκBβ and IKKγ-dominant-interfering mutants and kinase-deficient IKKα, IKKβ and NF-κB-inducing kinase mutants on Tax-mediated activation of the AID promoter. Jurkat cells were transfected with 0.9P (5 μg) together with Tax (10 μg) and the indicated DN mutants or empty vector (5 μg). (**D**) Functional effects of CREB DN mutants on Tax-mediated activation of AID promoter. Jurkat cells were transfected with 0.9P (5 μg) together with Tax (10 μg) and KCREB, CREB133 or empty vector (5 μg). Cells were harvested 48 h after transfection, and luciferase activity was measured with a luminometer. The results are expressed as fold induction by Tax or Tax mutants relative to the vector alone. Data are mean ± SD of three independent transfection experiments.

activation. The dominant interfering mutants of IκBα, IκBβ and IKKγ and kinase-deficient mutants of IKKα, IKKβ and NF-κB-inducing kinase were tested for their ability to inhibit Tax-mediated transactivation of AID-driven reporter gene activity. The expression of these inhibitory mutants inhibited Tax-induced activation of AID promoter (Figure 3C), suggesting that signaling components involved in the activation of NF-κB are necessary for Tax transactivation of the AID promoter.

We also tested the potential role of CREB in modulating Tax-induced AID promoter activity. For this purpose, the dominant-negative CREB mutants KCREB and CREB133 were transfected into Jurkat cells with the AID promoter construct as well as an expression vector for Tax. KCREB contains mutations in its DNA-binding domain (40). CREB133 contains a Ser-to-Ala mutation corresponding to amino acid 133, and this mutation blocks CREB phosphorylation, thus preventing transcription (40). Compared with transfections of an empty vector, KCREB- and CREB133-expressing Jurkat cells showed little Tax-mediated induction of the AID promoter (Figure 3D), suggesting that CREB is also required for Tax-mediated AID promoter activation.

To determine which site(s) of the *AID* gene promoter is responsible for the direct Tax-induced activation, we used plasmid constructs containing the 5′-flanking region and first intron. Two regions (CR1 and CR2) are present in the first intron and two E-boxes, the consensus sequence for E2A binding are present in the CR2 region (34). As shown in Figure 4A, 0.9P (promoter only), 0.9P-CR1+CR2 (promoter plus CR1 and CR2 fragments), 0.9P-CR1+CR2ΔE (promoter plus CR1 and CR2 fragments with deleted E-boxes) and 0.9P+I (promoter plus first intron) responded to Tax, suggesting the presence of a Tax-responsive element in the 5′-flanking region of the *AID* gene. To further delineate the Tax-responsive element within this region, we used various deletion constructs. As shown in Figure 4A, the 0.02P promoter lost the responsiveness to Tax, indicating that a Tax-responsive element may exist between −121 and −21 bp from the initiation site. We found one NF-κB-binding site, GGGAGGAGCC, which differed from the consensus sequence in two bases within this region and analyzed the promoter activity of the construct with deletion of this site (Figure 4B). The deletion reduced the response of the gene promoter to Tax activation. A residual transactivation by Tax hints to a minor contribution of other transcription factors including CREB. Thus, the NF-κB site seems to be the major element responsible for Tax-induced activation of *AID* gene.

HTLV-1 and Tax elicit NF-κB subunit binding to the AID NF-κB element

In the next step, we determined whether HTLV-1 infection induces NF-κB binding to the NF-κB element in the AID promoter. EMSA was performed with double-stranded oligonucleotides representing the NF-κB element. Compared with the control uninfected T-cell lines and ATL-derived T cell lines, protein complexes bound to the NF-κB site were detected in nuclear extracts from all HTLV-1-transformed T-cell lines examined at high levels (Figure 5A, left). Furthermore, protein complexes bound to the NF-κB element were detected in nuclear extracts from primary ATL cells but not normal PBMCs (Figure 5B, left).

The specificity of DNA–protein complex formation was determined by competition studies with unlabeled competitors. As

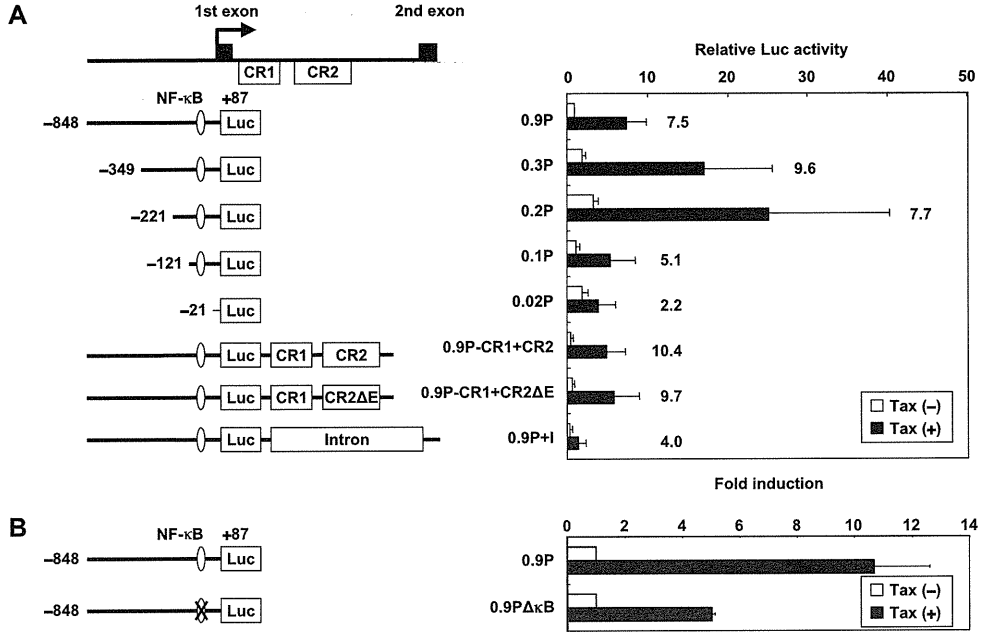

Fig. 4. Analysis of the *AID* gene promoter element required for Tax-induced activation. (**A**) Schematic diagrams of reporter constructs containing promoter only (0.9P), various promoter deletions (0.3P, 0.2P, 0.1P and 0.02P), all the conserved sequences (0.9P-CR1+CR2), all the conserved sequences with deleted E-boxes (0.9P-CR1+CR2ΔE) and promoter with intron (0.9P+I; left). The numbers on the AID promoter-luciferase complementary DNA constructs indicate the 5′-end points of the promoter sequence. Jurkat cells were transfected with various AID-luciferase constructs (5 μg) together with Tax (10 μg). The activities are expressed relative to that of cells transfected with 0.9P and an empty vector, which was defined as 1. The induction values represent the calculated values. (**B**) Tax transactivation of the NF-κB site deletion mutant of the AID promoter. Schematic representations of the AID promoter containing the wild-type (0.9P) and internal deletion mutant of the NF-κB site (0.9PΔκB). Jurkat cells were transfected with the indicated promoter constructs (5 μg) together with Tax (10 μg). Luciferase activity was analyzed, and the fold induction of Tax activity was calculated relative to the empty vector. Data are mean ± SD of three independent transfection experiments.

expected, a 100-fold molar excess of 'cold' AID NF-κB double-stranded oligonucleotides effectively competed with the labeled probe and eliminated the binding of nuclear extracts from MT-2 cells and primary ATL cells (Figure 5A and B, right, lanes 1 and 2). An unlabeled IL-8 AP-1 probe could not compete with a labeled probe (Figure 5A and B, right, lanes 1 and 4). Interestingly, a consensus NF-κB site from the IL-2 receptor α chain promoter could not also compete with the probe (Figure 5A and B, right, lanes 1 and 3). The exact composition of the transcription factor DNA–protein complexes in HTLV-1-infected T cells was ascertained by supershift analysis. Supershift reactions performed using MT-2 nuclear extracts indicated that p50 was the predominant component of the NF-κB complexes in MT-2 cells (Figure 5A, right, lane 5).

Nuclear extracts from JPX-9 cells also showed that Tax expression alone elicited binding to the AID NF-κB probe (Figure 5C, top). Induction of Tax expression resulted in the formation of a complex with the AID probe within 4 h, and this complex was eliminated by competition with a 100-fold molar excess of unlabeled AID NF-κB oligonucleotides but not by an IL-2 receptor α chain NF-κB and an AP-1 (Figure 5C, bottom, lanes 2–5). These results suggest that HTLV-1 infection and Tax expression result in the binding of the NF-κB complex to the NF-κB element of the AID promoter and that this complex differed from the NF-κB complex bound to the consensus NF-κB site.

To examine whether this site can bind p50 protein, recombinant p50 protein was analyzed by EMSA. Incubation of AID NF-κB oligonucleotides with the recombinant p50 produced a specific retarded complex (Figure 5D, lane 1) that could be inhibited by preincubation with a 100-fold molar excess of unlabeled NF-κB oligonucleotides but not by AP-1 (Figure 5D, lanes 1–5). The specific retarded complexes formed with recombinant p50 was supershifted with p50 antibody but not with p65 antibody (Figure 5D, lanes 6 and 7), indicating that this site is capable of binding p50 protein.

AID expression is regulated mainly by NF-κB activity

Based on the above results, it was intriguing to examine whether exogenous expression of subunits of NF-κB activate the AID promoter. Introduction of the p50 but not p65 subunit activated the AID promoter (Figure 5E), suggesting that activation of AID promoter by Tax is mediated by NF-κB p50 pathway.

To provide further evidence for the role of p50 in the signal transduction pathway leading to Tax-induced AID expression, the use of siRNA to suppress p50 decreased the expression of AID mRNA (Figure 5F, left) and NF-κB DNA binding (Figure 5F, right). In contrast, p65 siRNA did not inhibit the expression of AID (Figure 5F, middle). Next, we examined the Tax-mediated AID expression with NF-κB signaling inhibitors. We found that the NF-κB inhibitory reagents, *N*-acetyl-L-leucyl-L-leucyl-L-norleucinal [a proteasome inhibitor; (41)] and Bay 11-7082 [an inhibitor of IκBα phosphorylation; (42)] significantly suppressed AID mRNA expression (Figure 5G). Taken together, these findings indicate that the Tax-induced AID expression in T cells is mediated mainly through the activation of NF-κB.

HTLV-1-infected T cells express the transcriptional coactivator Bcl-3 that complexes with p50

The p50 homodimer binds DNA *in vitro*, but lacks a transcriptional activation domain and, consequently, initiates a weak, if any, transcription. In fact, this NF-κB homodimer appears to function as a transcriptional inhibitor in some cell types by competing with p50/p65 for promoter binding (43). Countering this inhibitory effect in a variety of transformed cell types is the oncoprotein Bcl-3, which binds p50 homodimers and robustly coactivates transcription (44). Experiments were thus conducted to explore the potential role of Bcl-3 in p50 transcriptional coactivation in HTLV-1-infected T cells. RT–PCR and western blots demonstrated high expression levels of Bcl-3 mRNA and protein in HTLV-1-infected T-cell lines compared with

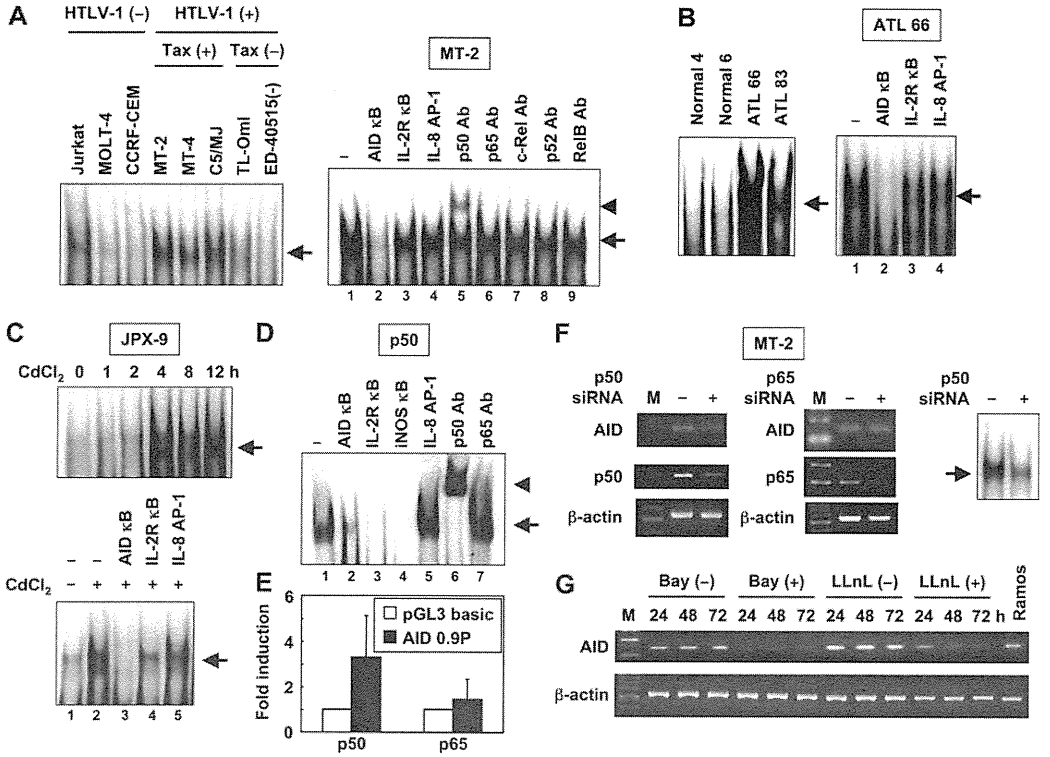

Fig. 5. p50 contributes to AID expression. (**A** and **B**) HTLV-1 infection is associated with binding of NF-κB factors to the NF-κB site in AID promoter. Nuclear extracts (5 μg) from control uninfected and HTLV-1-infected T-cell lines (**A**) and PBMCs from healthy volunteers and patients with ATL (**B**) were incubated with the labeled double-stranded oligonucleotides representing the AID NF-κB site in EMSA reactions. Nuclear extracts from MT-2 (**A**, right) and ATL (**B**, right) cells were subjected to competition analysis with a 100-fold molar excess of unlabeled double-stranded oligonucleotides representing the AID NF-κB site (lane 2), a consensus NF-κB site from the IL-2 receptor α chain (IL-2Rα) promoter (lane 3) or an AP-1 site from the IL-8 promoter (lane 4). The indicated unlabeled oligonucleotides were incubated with nuclear extracts for 15 min before binding reactions. Nuclear extracts from MT-2 cells were also subjected to supershift assays with either no antibody (lane 1) or the indicated antibodies (Abs; lanes 5–9). The Abs were incubated with nuclear extracts for 45 min before binding reactions. Arrows: the specific complexes, arrowheads: the DNA binding complexes supershifted by Abs. (**C**) Tax-induced NF-κB-binding activity. Nuclear extracts from JPX-9 cells treated with $CdCl_2$ (20 μM) for the indicated time periods were incubated with the labeled double-stranded oligonucleotides representing the AID NF-κB site (top). Nuclear extracts from JPX-9 cells treated with $CdCl_2$ (20 μM) for 4 h were subjected to competition analysis with a 100-fold molar excess of unlabeled double-stranded oligonucleotides representing the AID NF-κB site (lane 3), a consensus NF-κB site from the IL-2α promoter (lane 4) and an AP-1 site from the IL-8 promoter (lane 5). (**D**) Recombinant NF-κB subunit p50 was subjected to EMSA using the labeled double-stranded oligonucleotides representing the AID NF-κB site. Binding reaction was carried out in the presence of the indicated competitors (lanes 2–5). Lane 1, DNA complex in the absence of any competitor. In addition, incubation with antibody to p50 (lane 6) but not p65 (lane 7) supershifted the complex. Arrows: the specific complexes, arrowheads: the DNA-binding complexes supershifted by Abs. (**E**) Effect of overexpression of p50 and p65 on AID promoter. Jurkat cells were transfected with an expression plasmid for either p50 or p65 component of NF-κB (5 μg) along with either pGL3 basic or AID 0.9P (5 μg). Luciferase activity was analyzed, and the fold induction of p50 or p65 activity was calculated relative to the empty vector. Data are mean ± SD of three independent transfection experiments. (**F**) Suppression of endogenous p50 reduces the expression of AID mRNA and NF-κB DNA binding. MT-2 cells were transfected with either p50 or control siRNA and either p65 or control siRNA. At 48 h after transfection, total RNA was isolated from each cell, and the expression levels of p50, p65, AID and β-actin (loading control) mRNAs were measured by RT–PCR. Nuclear extracts were also isolated from each cell and subjected to EMSA with the AID NF-κB probe (right). (**G**) Effects of NF-κB inhibitors on endogenous AID expression in an HTLV-1-infected T cell line. MT-2 cells were treated with either Bay 11-7082 (10 μM) or *N*-acetyl-L-leucyl-L-leucyl-L-norleucinal (20 μM) for the indicated time periods. Total RNA was isolated from each cell, and the AID mRNA expression level was measured by RT–PCR.

uninfected T-cell lines (Figure 6A). Treatment of JPX-9 cells with $CdCl_2$ induced Tax expression (Figures 2C and 6B) and also enhanced the expression levels of Bcl-3 mRNA and protein (Figure 6B), suggesting that Tax upregulates Bcl-3 expression. Immunofluorescent staining and confocal microscopy showed colocalization of Bcl-3 and p50 proteins in nuclei of MT-2 cells (Figure 6C). Next, we examined the association between Bcl-3 and p50 in HTLV-1-infected T cells. Proteins from MT-2 cell lysates were immunoprecipitated with rabbit IgG or anti-Bcl-3 antibody, followed by western blotting with antibody to p50. p50 was identified in Bcl-3 immunoprecipitates (Figure 6D, left). In addition, cell extracts from MT-2 cells were immunoprecipitated with rabbit IgG or anti-p50 antibody, and the presence of Bcl-3 in the complex was analyzed by western blotting. Figure 6D, right panels show that Bcl-3 was coimmunoprecipitated with p50, indicating the presence of Bcl-3/p50 complexes in HTLV-1-infected T cells, with the potential for transcriptional activity.

Finally, we examined the expression levels of AID, Bcl-3 and Tax mRNA in primary ATL cells. As shown in Figure 6E, ATL cells constitutively expressed Bcl-3 mRNA, but ATL cells from not all patients expressed AID mRNA. AID mRNA expression did not correlate with that of Tax. Although we could not examine protein complexes bound to the NF-κB site in these cells, activation of p50/Bcl-3 complexes might explain the expression of AID in primary ATL cells.

Discussion

The involvement of AID in the progression of leukemia has been suggested based on the correlation between AID expression and poor prognosis of patient with B-cell chronic lymphocytic leukemia (45,46). However, a simple correlation does not tell us whether AID expression is the cause or the result of leukemia. On the other hand, a causal relationship was suggested in a study of AID transgenic mice

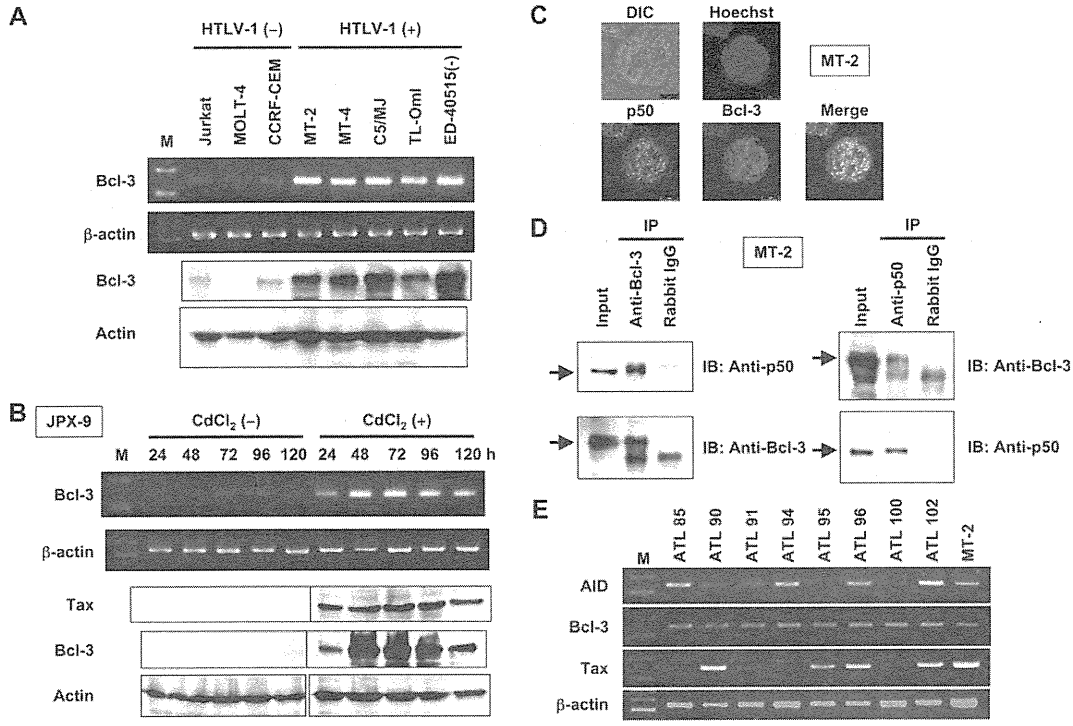

Fig. 6. HTLV-1-infected T cells express Bcl-3/p50 complexes. (**A**) Expression of Bcl-3 in HTLV-1-infected T-cell lines. RT–PCR analysis was carried out for Bcl-3 and β-actin (loading control). Western blot analysis was performed for Bcl-3 and actin. (**B**) Induction of Bcl-3 expression by Tax. JPX-9 cells were treated with or without 20 μM of $CdCl_2$ for the indicated time periods. RT–PCR was carried out for Bcl-3 and β-actin (loading control). Western blot analysis was also performed for Tax, Bcl-3 and actin (loading control). (**C**) Immunofluorescence images of MT-2 cells for p50 (Alexa Fluor 488; green), Bcl-3 (Alexa Fluor 546; red) and nuclei (Hoechst 33342; blue). p50 colocalizes with Bcl-3 *in situ* in the nuclei of MT-2 cells; DIC, differential interference contrast. (**D**) Cell lysates from MT-2 cells were used for immunoprecipitation with anti-Bcl-3 or anti-p50 antibody followed by immunoblotting with anti-p50 or anti-Bcl-3 antibody. The expression level of p50 or Bcl-3 was detected (input). (**E**) RT–PCR analysis for AID, Bcl-3 and Tax expression in primary ATL cells.

(13). These mice spontaneously and frequently develop T-cell lymphoma and lung microadenoma in association with high mutation frequencies. The reason for T cells and the lung epithelium to be the targets of cancer formation in AID transgenic mice, despite the ubiquitous expression of AID is unknown at present. Nonetheless, the fact that aberrant AID expression in mice led to T-cell lymphoma suggests that AID could be the cause of T-cell neoplasm.

In the present study, we examined AID expression in HTLV-1-infected T-cell lines and primary ATL cells and compared the expression level with that in uninfected T-cell lines from T-ALL patients and normal PBMCs. The results showed that HTLV-1-transformed T-cell lines (3/3) and ATL cells from 14 of 18 patients expressed significantly higher levels of AID than did any other cells. Furthermore, the cytoplasmic AID expression was confirmed by immunohistochemistry in primary ATL cells invading skin tissues (10/10) and lymph nodes (6/6). However, AID expression was negative in T-ALL (2/2) and positive in only one sample in six B-ALL ones. The G to A mutations (e.g. Arg273His and Gly245Asp) of the *p53* gene were reported in primary ATL cells (47), suggesting that AID could target the *p53* gene in ATL.

One important finding of this study was that HTLV-1 and viral transforming protein Tax triggered aberrant AID expression in T cells. Indeed, AID expression correlated with that of Tax in T-cell lines. Furthermore, we identified AID as a target gene of the NF-κB and CREB activation pathways in T cells. Since we did not identify the putative binding elements for CREB between −121 and −21 bp from AID promoter sequence analyses, CREB is probably not directly involved in Tax-induced AID expression. Alternatively, these results suggest the involvement of a Tax-response element different from the known CRE site. The presence of p50 but not p65 in the NF-κB DNA complexes of the AID promoter in HTLV-1-infected T cells is an intriguing finding. This NF-κB subtype may be involved in the competitive transcriptional inhibition of p50/p65, a function frequently attributed to the p50 homodimer (43). However, the expression of the transcriptional coactivator Bcl-3 in the HTLV-1-infected T-cell line, and the complexing of Bcl-3 with p50, provides preliminary evidence suggesting that the p50 homodimers may be transcriptionally active. The oncoprotein Bcl-3 is a member of the IκB family of NF-κB binding proteins. The *BCL3* gene, located on chromosome 19, is translocated intact and is activated in cases of t(14;19)(q32.3;q13.2) B-cell chronic lymphocytic leukemia (48). Bcl-3 has been implicated also in the pathogenesis of nasopharyngeal carcinoma, breast cancer and a variety of lymphomas, all cases giving evidence for coactivation of NF-κB p50 by Bcl-3 as the transforming event (44,49–51). Bcl-3 expression and its interaction with NF-κB p50 have not been previously reported in HTLV-1-infected T cells, although Tax is known to associate with Bcl-3 and induce Bcl-3 expression (52,53). It is interesting to speculate that Bcl-3/p50 complexes may be important in the transcription of mutation inducing gene *AID*. Tax induces Bcl-3 expression through stimulation of the NF-κB pathway (53), suggesting that *AID* gene is the primary and secondary target of Tax-induced NF-κB activation. Bcl-3 also functions as a repressor of transcription from the HTLV-1 long terminal repeat (52,53). Bcl-3 may promote somatic mutation frequency through the induction of AID and may attenuate virus production, facilitating immune evasion.

It is known that after the early phase of HTLV-1 infection, Tax expression is repressed *in vivo*, probably due to immune surveillance. Tax-negative ATL-derived T-cell lines, TL-OmI and ED-40515(-), did not express AID, but primary ATL cells expressed AID. Interestingly, Tax-expressing cells and primary ATL cells had higher levels of the protein complexes bound to the NF-κB element in the AID promoter compared with Tax-negative ATL-derived T-cell lines. Since the expression of Tax in some primary ATL cells was only detected by RT–PCR (Figure 6E), a trace amount of Tax seems to be sufficient for

the induction of AID in ATL cells. However, Tax-negative ATL cells (ATL 85 and 94) expressed AID mRNA at the relatively high levels. Alternatively, NF-κB activation might be necessary for the constitutive expression of AID. It is thus reasonable to assume that transactivation by Tax is not the only mechanism underlying overexpression of AID in ATL cells.

In conclusion, our findings provide the first evidence that AID is induced in response to Tax via the Bcl-3/NF-κB signaling pathway and might be involved in the development of ATL. However, there is room for further investigation to determine whether aberrant AID expression could contribute to the accumulation of genomic mutations in T cells. Recently, induction of reactive oxygen species by Tax has been reported to elicit DNA damage (54). Initiation of DNA double-strand break formation by AID requires reactive oxygen species intermediates, such as hydroxy radicals (55). Tax could make structural DNA changes both through enzymes such as AID and through reactive oxygen species. Understanding the mechanisms of AID upregulation in T cells might provide a new strategy to prevent the development and progression of ATL. The constitutive expression of mutator enzyme AID in ATL cells can be speculated to result from mutations induced by the Tax-activated AID and/or other Tax-associated mutagenic mechanisms during the pre-leukemic stage.

Funding

This work was supported in part by Japan Leukemia Research Fund to NM and Osaka Cancer Research Foundation to N.M.

Acknowledgements

We thank the many patients with ATL and ALL and the control subjects who donated samples for these studies. We acknowledge Drs Shigeki Sawada and Tetsuro Nakazato and Mr Yukimasa Shibata for the expert technical assistance. We thank Drs Taeko Okudaira, Jun-Nosuke Uchihara, Naoya Taira, Kazuiku Ohshiro, Takehiro Matsuda, Hiroshi Uezato and Koichi Ohshima for providing patient samples. We thank Drs Kayoko Matsumoto, Dean W.Ballard, Romas Geleziunas and Kuan-Teh Jeang for providing expression vectors for Tax and its mutants; for IκBα and IκBβ-dominant-negative mutants; for NF-κB-inducing kinase, IKKα and IKKβ-dominant-negative mutants and for IKKγ-dominant-negative mutant. We thank Dr Masataka Nakamura for providing JPX-9, Dr Michiyuki Maeda for providing ED-40515(-) and Fujisaki Cell Center, Hayashibara Biomedical Laboratories (Okayama, Japan) for providing the C5/MJ cell line. We also thank Dr Yuetsu Tanaka for providing Tax monoclonal antibody. Recombinant human IL-2 was kindly provided by Takeda Chemical Industries (Osaka, Japan).

Conflict of Interest Statement: None declared.

References

1. Yoshida,M. *et al.* (1982) Isolation and characterization of retrovirus from cell lines of human adult T-cell leukemia and its implication in the disease. *Proc. Natl Acad. Sci. USA*, **79**, 2031–2035.
2. Matsuoka,M. *et al.* (2007) Human T-cell leukaemia virus type 1 (HTLV-1) infectivity and cellular transformation. *Nat. Rev. Cancer*, **7**, 270–280.
3. Grassmann,R. *et al.* (2005) Molecular mechanisms of cellular transformation by HTLV-1 Tax. *Oncogene*, **24**, 5976–5985.
4. Jin,D.-Y. *et al.* (1998) Human T cell leukemia virus type 1 oncoprotein Tax targets the human mitotic checkpoint protein MAD1. *Cell*, **93**, 81–91.
5. Majone,F. *et al.* (2000) Clastogenic effect of the human T-cell leukemia virus type I Tax oncoprotein correlates with unstabilized DNA breaks. *J. Biol. Chem.*, **275**, 32906–32910.
6. Marriott,S.J. *et al.* (2002) Damaged DNA and miscounted chromosomes: human T cell leukemia virus type I tax oncoprotein and genetic lesions in transformed cells. *J. Biomed. Sci.*, **9**, 292–298.
7. Azran,I. *et al.* (2004) Role of Tax protein in human T-cell leukemia virus type-I leukemogenicity. *Retrovirology*, **1**, 20.
8. Vogelstein,B. *et al.* (2004) Cancer genes and the pathways they control. *Nat. Med.*, **10**, 789–799.
9. Kinoshita,K. *et al.* (2006) The dark side of activation-induced cytidine deaminase: relationship with leukemia and beyond. *Int. J. Hematol.*, **83**, 201–207.
10. Marusawa,H. (2008) Aberrant AID expression and human cancer development. *Int. J. Biochem. Cell. Biol.*, **40**, 1399–1402.
11. Honjo,T. *et al.* (2002) Molecular mechanism of class switch recombination: linkage with somatic hypermutation. *Ann. Rev. Immunol.*, **20**, 165–196.
12. Yoshikawa,K. *et al.* (2002) AID enzyme-induced hypermutation in an actively transcribed gene in fibroblasts. *Science*, **296**, 2033–2036.
13. Okazaki,I.-M. *et al.* (2003) Constitutive expression of AID leads to tumorigenesis. *J. Exp. Med.*, **197**, 1173–1181.
14. Endo,Y. *et al.* (2007) Expression of activation-induced cytidine deaminase in human hepatocytes via NF-κB signaling. *Oncogene*, **26**, 5587–5595.
15. Matsumoto,Y. *et al.* (2007) *Helicobacter pylori* infection triggers aberrant expression of activation-induced cytidine deaminase in gastric epithelium. *Nat. Med.*, **13**, 470–476.
16. Miyoshi,I. *et al.* (1981) Type C virus particles in a cord T-cell line derived by co-cultivating normal human cord leukocytes and human leukaemic T cells. *Nature*, **294**, 770–771.
17. Yamamoto,N. *et al.* (1982) Transformation of human leukocytes by cocultivation with an adult T cell leukemia virus producer cell line. *Science*, **217**, 737–739.
18. Popovic,M. *et al.* (1983) Isolation and transmission of human retrovirus (human T-cell leukemia virus). *Science*, **219**, 856–859.
19. Sugamura,K. *et al.* (1984) Cell surface phenotypes and expression of viral antigens of various human cell lines carrying human T-cell leukemia virus. *Int. J. Cancer*, **34**, 221–228.
20. Maeda,M. *et al.* (1985) Origin of human T-lymphotrophic virus I-positive T cell lines in adult T cell leukemia: analysis of T cell receptor gene rearrangement. *J. Exp. Med.*, **162**, 2169–2174.
21. Ohtani,K. *et al.* (1989) Electroporation: application to human lymphoid cell lines for stable introduction of a transactivator gene of human T-cell leukemia virus type I. *Nucleic Acids Res.*, **17**, 1589–1604.
22. Hieshima,K. *et al.* (2008) Tax-inducible production of CC chemokine ligand 22 by human T cell leukemia virus type 1 (HTLV-1)-infected T cells promotes preferential transmission of HTLV-1 to CCR4-expressing $CD4^+$ T cells. *J. Immunol.*, **180**, 931–939.
23. Brenner,C.A. *et al.* (1989) Message amplification phenotyping (MAPPing): a technique to simultaneously measure multiple mRNAs from small numbers of cells. *Biotechniques*, **7**, 1096–1103.
24. Oettinger,R. *et al.* (1999) Production of reactive oxygen intermediates by human macrophages exposed to soot particles and asbestos fibers and increases in NF-kappa B p50/p105 mRNA. *Lung*, **177**, 343–354.
25. Elliott,S.F. *et al.* (2002) Bcl-3 is an interleukin-1-responsive gene in chondrocytes and synovial fibroblasts that activates transcription of the matrix metalloproteinase 1 gene. *Arthritis Rheum.*, **46**, 3230–3239.
26. Lin,H. *et al.* (2009) Primary culture of human blood-retinal barrier cells and preliminary study of APOBEC3 expression: an in vitro study. *Invest. Ophthalmol. Vis. Sci.*, **50**, 4436–4443.
27. Tanaka,Y. *et al.* (1990) Heterogeneity of antigen molecules recognized by anti-tax1 monoclonal antibody Lt-4 in cell lines bearing human T cell leukemia virus type I and related retroviruses. *Jpn. J. Cancer Res.*, **81**, 225–231.
28. Yoshida,T. *et al.* (2001) IL-2 independent transformation of a unique human T cell line, TY8-3, and its subclones by HTLV-I and -II. *Int. J. Cancer*, **91**, 99–108.
29. Matsumoto,K. *et al.* (1997) Human T-cell leukemia virus type 1 Tax protein transforms rat fibroblasts via two distinct pathways. *J. Virol.*, **71**, 4445–4451.
30. Brockman,J.A. *et al.* (1995) Coupling of a signal response domain in IκBα to multiple pathways for NF-κB activation. *Mol. Cell. Biol.*, **15**, 2809–2818.
31. McKinsey,T.A. *et al.* (1996) Inactivation of IκBβ by the Tax protein of human T-cell leukemia virus type 1: a potential mechanism for constitutive induction of NF-κB. *Mol. Cell. Biol.*, **16**, 2083–2090.
32. Geleziunas,R. *et al.* (1998) Human T-cell leukemia virus type 1 Tax induction of NF-κB involves activation of the IκB kinase α (IKKα) and IKKβ cellular kinases. *Mol. Cell. Biol.*, **18**, 5157–5165.
33. Iha,H. *et al.* (2003) Segregation of NF-κB activation through NEMO/IKKγ by Tax and TNFα: implications for stimulus-specific interruption of oncogenic signaling. *Oncogene*, **22**, 8912–8923.
34. Gonda,H. *et al.* (2003) The balance between Pax5 and Id2 activities is the key to AID gene expression. *J. Exp. Med.*, **198**, 1427–1437.

35. Mori,N. *et al.* (1996) Transactivation of the interleukin-1α promoter by human T-cell leukemia virus type I and type II Tax proteins. *Blood*, **87**, 3410–3417.
36. Chiu,Y.L. *et al.* (2008) The APOBEC3 cytidine deaminases: an innate defensive network opposing exogenous retroviruses and endogenous retroelements. *Ann. Rev. Immunol.*, **26**, 317–353.
37. Matsuda,T. *et al.* (2005) Human T cell leukemia virus type I-infected patients with Hashimoto's thyroiditis and Graves' disease. *J. Clin. Endocrinol. Metab.*, **90**, 5704–5710.
38. Teruya,H. *et al.* (2008) Human T-cell leukemia virus type I infects human lung epithelial cells and induces gene expression of cytokines, chemokines and cell adhesion molecules. *Retrovirology*, **5**, 86.
39. Koiwa,T. *et al.* (2002) 5'-long terminal repeat-selective CpG methylation of latent human T-cell leukemia virus type 1 provirus *in vitro* and *in vivo*. *J. Virol.*, **76**, 9389–9397.
40. Amorino,G.P. *et al.* (2003) Dominant-negative cAMP-responsive element-binding protein inhibits proliferating cell nuclear antigen and DNA repair, leading to increased cellular radiosensitivity. *J. Biol. Chem.*, **278**, 29394–29399.
41. Jeremias,I. *et al.* (1998) Inhibition of nuclear factor κB activation attenuates apoptosis resistance in lymphoid cells. *Blood*, **91**, 4624–4631.
42. Pierce,J.W. *et al.* (1997) Novel inhibitors of cytokine-induced IκBα phosphorylation and endothelial cell adhesion molecule expression show anti-inflammatory effects *in vivo*. *J. Biol. Chem.*, **272**, 21096–21103.
43. Plaksin,D. *et al.* (1993) KBF1 (p50 NF-kappa B homodimer) acts as a repressor of H-2Kb gene expression in metastatic tumor cells. *J. Exp. Med.*, **177**, 1651–1662.
44. Fujita,T. *et al.* (1993) The candidate proto-oncogene *bcl-3* encodes a transcriptional coactivator that activates through NF-κB p50 homodimers. *Genes Dev.*, **7**, 1354–1363.
45. Oppezzo,P. *et al.* (2003) Chronic lymphocytic leukemia B cells expressing AID display dissociation between class switch recombination and somatic hypermutation. *Blood*, **101**, 4029–4032.
46. McCarthy,H. *et al.* (2003) High expression of activation-induced cytidine deaminase (AID) and splice variants is a distinctive feature of poor-prognosis chronic lymphocytic leukemia. *Blood*, **101**, 4903–4908.
47. Sakashita,A. *et al.* (1992) Mutations of the p53 gene in adult T-cell leukemia. *Blood*, **79**, 477–480.
48. Ohno,H. *et al.* (1990) The candidate proto-oncogene *bcl-3* is related to genes implicated in cell lineage determination and cell cycle control. *Cell*, **60**, 991–997.
49. Cogswell,P.C. *et al.* (2000) Selective activation of NF-κB subunits in human breast cancer: potential roles for NF-κB2/p52 and for Bcl-3. *Oncogene*, **19**, 1123–1131.
50. Thornburg,N.J. *et al.* (2003) Activation of nuclear factor-κB p50 homodimer/Bcl-3 complexes in nasopharyngeal carcinoma. *Cancer Res.*, **63**, 8293–8301.
51. Mathas,S. *et al.* (2005) Elevated NF-κB p50 complex formation and Bcl-3 expression in classical Hodgkin, anaplastic large-cell, and other peripheral T-cell lymphomas. *Blood*, **106**, 4287–4293.
52. Hishiki,T. *et al.* (2007) BCL3 acts as a negative regulator of transcription from the human T-cell leukemia virus type 1 long terminal repeat through interactions with TORC3. *J. Biol. Chem.*, **282**, 28335–28343.
53. Kim,Y.-M. *et al.* (2008) The proto-oncogene Bcl3, induced by Tax, represses Tax-mediated transcription via p300 displacement from the human T-cell leukemia virus type 1 promoter. *J. Virol.*, **82**, 11939–11947.
54. Kinjo,T. *et al.* (2010) Induction of reactive oxygen species by human T-cell leukemia virus type 1 Tax correlates with DNA damage and expression of cellular senescence marker. *J. Virol.*, **84**, 5431–5437.
55. Guikema,J.E.J. *et al.* (2010) p53 represses class switch recombination to IgG2a through its antioxidant function. *J. Immunol.*, **184**, 6177–6187.

Received May 9, 2010; revised October 10, 2010; accepted October 19, 2010

OPEN ACCESS Freely available online

PLoS one

Increased Risk of Temporomandibular Joint Closed Lock: A Case-Control Study of ANKH Polymorphisms

Boyen Huang[1], Katsu Takahashi[1]*, Tomoko Sakata[1], Honoka Kiso[1], Manabu Sugai[2], Kazuma Fujimura[1], Akira Shimizu[2], Shinji Kosugi[3], Tosiya Sato[4], Kazuhisa Bessho[1]

1 Department of Oral and Maxillofacial Surgery, Graduate School of Medicine, Kyoto University, Kyoto, Japan, **2** Translational Research Center, Kyoto University Hospital, Kyoto University, Kyoto, Japan, **3** Department of Biomedical Ethics, Graduate School of Medicine, Kyoto University, Kyoto, Japan, **4** Department of Biostatistics, School of Public Health, Kyoto University, Kyoto, Japan

Abstract

Objectives: This study aimed to carry out a histological examination of the temporomandibular joint (TMJ) in *ank* mutant mice and to identify polymorphisms of the human ANKH gene in order to establish the relationship between the type of temporomandibular disorders (TMD) and ANKH polymorphisms.

Materials and Methods: Specimens from the TMJ of *ank* mutant and wild-type mice were inspected with a haematoxylin and eosin staining method. A sample of 55 TMD patients were selected. Each was examined with standard clinical procedures and genotyping techniques.

Results: The major histological finding in *ank* mutant mice was joint space narrowing. Within TMD patients, closed lock was more prevalent among ANKH-OR homozygotes ($p = 0.011$, OR = 7.7, 95% CI 1.6–36.5) and the elder ($p = 0.005$, OR = 2.4, 95% CI 1.3–4.3).

Conclusions: Fibrous ankylosis was identified in the TMJ of *ank* mutant mice. In the human sample, ANKH-OR polymorphism was found to be a genetic marker associated with TMJ closed lock. Future investigations correlating genetic polymorphism to TMD are indicated.

Citation: Huang B, Takahashi K, Sakata T, Kiso H, Sugai M, et al. (2011) Increased Risk of Temporomandibular Joint Closed Lock: A Case-Control Study of ANKH Polymorphisms. PLoS ONE 6(10): e25503. doi:10.1371/journal.pone.0025503

Editor: Alejandro Almarza, University of Pittsburgh, United States of America

Received March 24, 2011; **Accepted** September 6, 2011; **Published** October 7, 2011

Funding: This study was supported by a JSPS (official website: http://www.jsps.go.jp/english/) Postdoctoral Fellowship for Foreign Researchers (P09741) and a Grant-in-Aid for Scientific Research (B) from Japanese Society for the Promotion of Science. The funders had no role in study design, data collection and analysis, decision to publish, or preparation of the manuscript.

Competing Interests: The authors have declared that no competing interests exist.

* E-mail: takahask@kuhp.kyoto-u.ac.jp

Introduction

Temporomandibular disorders (TMD) are a developing issue in public health with clinical signs being observed in 50% of the population [1,2]. Analysis of data derived from clinical records has found that the majority of symptomatic TMD patients exhibited internal derangement of the temporomandibular joint (TMJ) [3]. Treatment outcomes of TMJ internal derangement remain controversial although various management options such as arthroscopy, arthrocentesis and physiotherapy have been suggested [4–6].

Internal derangement has been associated with 90% of cases suffering from TMJ closed lock [4]. Closed lock was identified as a permanently displaced disc and direct condyle articulation against a vascularised posterior disc attachment [7]. This manifestation generally emerged as a progression from TMJ clicking, pain and/or intermittent locking [4]. Although internal derangement was found to be preceded by TMJ clicking [4], TMJ clicking did not predispose closed lock [8]. TMJ clicking and closed lock showed contrasting tissue reactions [7]. The conditions also differed in their correlations to Type I TMJ ankylosis [9], a disorder characterised by articular fibrous adhesions in the TMJ [10]. In addition, compared to the cases with TMJ clicking, those that had progressed to closed lock were more likely accompanied with osteoarthritis [11]. These findings implied a pathological divergence between closed lock and TMJ clicking.

The over-expression of certain genes such as lumican [12], TRAIL and DR5 [13] has been detected in TMJ discs exhibiting internal derangement. A nonsynonymous mutation of the COMT gene was identified in a patient with TMJ closed lock [14]. In spite of these early findings, genetic influences on TMJ internal derangement require further investigation. In further research, a higher frequency of TMJ internal derangement and degenerative changes has been reported in patients with ankylosing spondylitis [15]. Recent studies have proposed *ank* mutations and ANKH polymorphisms, respectively, as determinants for arthritis in mice [16] and ankylosing spondylitis in humans [17]. The ANKH gene is a human homolog of the murine progressive ankylosis gene, *ank* [17]. Although the TMJ was susceptible to the above ANKH-related diseases [15,18,19], the connection between TMD and the ANKH gene remains unknown.

Since genetic effects on TMJ internal derangement have not been fully clarified and the progressive ankylosis gene was associated with joint disorders, an investigation of this gene may

help to gain insights into the pathogenesis of TMD. Therefore, this study aimed (1) to carry out a histological examination of the TMJ collected from *ank* mutant as well as wild-type mice, and (2) to conduct a case-control research study to identify polymorphisms of the ANKH gene, using a sample of TMD patients in Japan. A special interest was to establish a relationship between the types of TMJ internal derangement and ANKH polymorphisms.

Materials and Methods

Prior to commencement, animal and human sub-projects of this study have both received appropriate ethics approval from the Institutional Review Board of Kyoto University (approved ID Number: G86). Commercially bred *ank/ank* mutant and wild-type mice (Jackson Laboratory, Bar Harbor, ME, USA, http://jaxmice.jax.org/strain/000200.html) were purchased for the animal experiment. The mice were separately euthanised with carbon dioxide gas at 3, 4 and 5 months of age, since the life span of *ank/ank* mutant mice was less than 6 months [20]. Tissues of the TMJ were collected and prepared. The number of tissue sections (8 μm) per TMJ ranged from 50 to 150. Every 5th sequenced section was examined with a haematoxylin and eosin staining (HE stain) method [21].

To identify the expression of ANKH in TMJ, an mRNA expression analysis was conducted. Synovial cells used for this purpose were collected from a patient undergoing TMJ arthroscopy due to closed lock, with appropriate written informed consent received. Procedures for preparation of the primary culture and the reverse transcriptase polymerase chain reaction (RT-PCR), as suggested in literature [22], were used. This study applied AnkRTF4 (5′-ATCAAGAAGTTCACCTTCGTC-3′) and AnkRTR4 (5′-CTTTTTCTGCTTCCGGTAGAC-3′) as the primers to perform the RT-PCR technique.

This study hypothesised that closed lock patients were more likely to carry a homozygous ANKH polymorphic genotype. The calculation of a minimal sample size based on the statistical power to hypothesis testing was unattainable, since the homozygosity/heterozygosity distribution of the ANKH polymorphisms studied has never been reported. The percentage of controls carrying a homozygous ANKH polymorphism would be required for estimating the sample size of such an unmatched case-control study. To achieve a satisfactory sample size for an adequate statistical power, sample collection was carried out from January 2003 to December 2006. A sample was recruited for the study at the outpatient clinic of oral and maxillofacial surgery, Kyoto University Hospital. Inclusion criteria for subjects of the study were: (1) having a Japanese ethnicity background; (2) being older than 15 years of age; (3) presenting signs and symptoms that were characteristic of a diagnosis of TMJ clicking (disc displacement with reduction) or closed lock (disc displacement without reduction) [23,24]; and (4) not having a previous history of trauma, neoplasm and/or surgery in the TMJ. The assessment consisted of a standardised clinical evaluation of mandibular range of motion, joint pain, joint sounds [23] and a magnetic resonance imaging (MRI) examination using a 1.5-T MRI scanner with bilateral 3-inch dual-surface coils (Signa, GE Healthcare, Little Chalfont, UK). Based on diagnoses, subjects were categorised as closed lock or TMJ clicking. Participants appearing with intermittent lock, a temporary and recurrent limitation of mouth opening [25], were excluded from the study, since proceeding developments of the indefinite manifestation ranged from a disc displacement with reduction to a complete disappearance of symptoms [25]. As absence of clicking sound failed to indicate a normal joint [25,26] and this study focused on comparison between the two types of internal derangement, TMJ clicking patients instead of asymptomatic individuals were used as the controls. Closed lock subjects, on the other hand, were used as the cases. Before inclusion, written informed consent was received from all patients. Clinical and demographic data of each participant, including the type of TMJ internal derangement (closed lock or clicking), age (years) and gender (male or female), were collected. Blood samples of the patients were obtained and then prepared for DNA isolation. Total genomic DNA from peripheral leukocytes was extracted with a QIAamp DNA Blood Midi Kit (QIAGEN, Hilden, Germany).

The genotyping techniques reported by a previous study were used to identify the ANKH-OR polymorphic site and the ANKH-TR polymorphic site in the 5′-noncoding region and the promoter region of the ANKH gene, respectively [17]. The polymerase chain reaction (PCR) procedure for genotyping was carried out with application of LA Taq with GC Buffer (TaKaRa, Tokyo, Japan). This was initiated with 30 cycles of 30-second denaturation at 94°C, followed by 30-second annealing at 60°C and 2-minute extension at 72°C, in a GeneAmp PCR System 9700 thermal cycler (Applied Biosystems, Foster City, CA, USA). After sequencing the isolated PCR products with a BigDye Terminator v1.1 Cycle Sequencing Kit (Applied Biosystems, Foster City, CA, USA), the sequencing reaction products were purified with a Centri-Sep Spin Column (Princeton Separations, Freehold, NJ, USA). Sequences of the sense and the antisense strands in the above products were then obtained, using a 3100 Genetic Analyzer (Applied Biosystems, Foster City, CA, USA). Thus, polymorphisms of the ANKH gene in each sample were detected. Based on combinations of alleles, the variables of genotypes studied included ANKH-OR (homozygotes or heterozygotes) and ANKH-TR (homozygotes or heterozygotes) polymorphisms. All procedures were carried out according to the manufacturers' instructions.

Data entry and statistical analysis were implemented with JMP 8.0 (SAS Institute Inc., Cary, NC, USA, 2008). Data analysis included descriptive statistics (frequency distribution and cross tabulation). A univariate logistic regression method was used to assess the individual (unadjusted) contribution of explanatory variables including genotypes of ANKH polymorphisms, gender and/or age [27]. Variables that showed statistical significance in the univariate analysis were selected to enter a multivariate logistic regression model to examine the collective (adjusted) effect [27]. As highly correlated variables included in a model together might lead to overestimation or understimation of their significance [27], correlated ANKH-OR and ANKH-TR [17] were separatedly added into two different models. The level of two-sided significance was set at 5%.

Results

In both the *ank/ank* mutant and the wild-type mice, six 3-month-olds, two 4-month-olds and two 5-month-olds were examined. Mutant individuals of all age groups showed similarly narrower and/or ankylosed superior and inferior synovial cavities filled with fibrous connective tissue throughout the entire joint space (Figure 1: A–C). This was not seen in any of the wild-type mice (Figure 1: D–F). Thicker fibrocartilage in the condylar head and inflammatory cell infiltration in the synovial membrane were identified in one (Figure 1: A–C) but not all *ank/ank* mutant mice. Osseous ankylosis, bone/cartilage erosion, calcified debris and joint calcification were not found in the TMJ of either genotype amongst any age groups. As for the human TMJ, the primary culture of cells derived from the surgically removed synovial membrane expressed ANKH at the mRNA level (Figure 2: A).

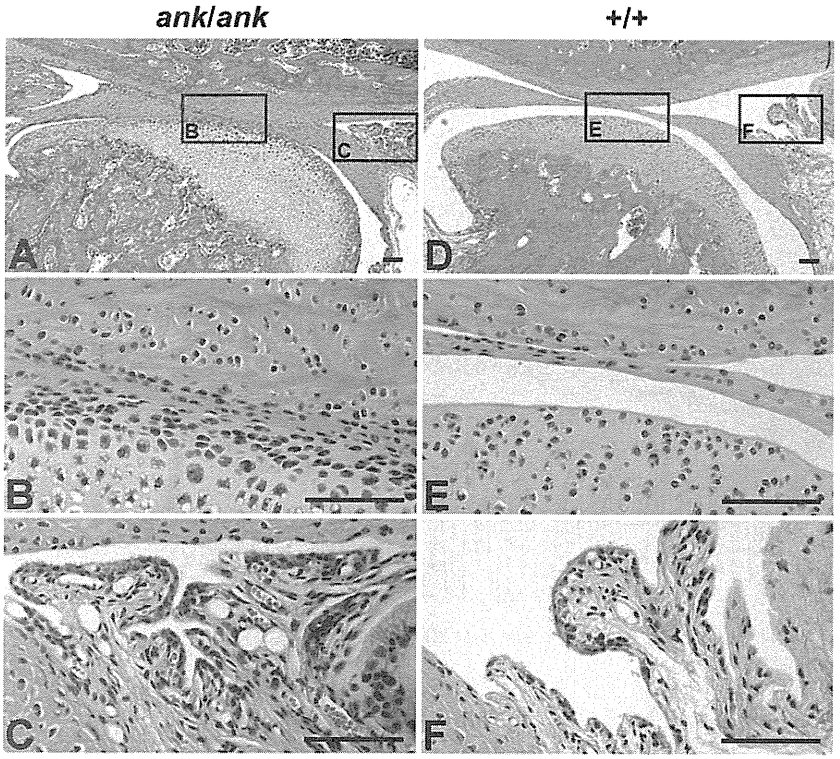

Figure 1. Representative HE stain photomicrographs of the TMJ from *ank/ank* mutant and wild-type mice. (A to C) Representative HE stain photomicrographs of the TMJ from a 3-month-old *ank/ank* mutant mouse of the study. (A) Narrower and/or ankylosed superior and inferior synovial cavities filled with fibrous connective tissue were visible. (B) A closer view of the ankylosed/adhered joint space. (C) Inflammatory cells appeared in the synovial membrane of one but not all mice. (D to F) Representative HE stain photomicrographs of the TMJ from a 3-month-old wild-type mouse of the study. (D) A normal and clear joint space was shown. (E) A closer view of the normal joint space. (F) The retrodiscal tissue was in a normal condition. Depth of tissue section in all photomicrographs: 3385 μm mesial to the most buccal point at the intersection of the zygomatic and the temporal bones. Scale bars in all photomicrographs: 100 μm.
doi:10.1371/journal.pone.0025503.g001

From January 2003 to December 2006, five-hundred-and-forty suspected cases of TMJ internal derangement attended the outpatient clinic of oral and maxillofacial surgery, Kyoto University Hospital. One-hundred-and-fifty-one patients completed both clinical and MRI examination sessions. Excluding 17 cases with an inconsistent diagnosis, internal derangement was confirmed by both assessments in a total of 134 patients. These included 61 cases with locking and 73 cases without locking but clicking. All of the 134 patients were from a Japanese ethinicity background, being older than 15 years of age, and having no previous history of trauma, neoplasm and/or surgery in the TMJ. Fifty-two locking cases and 16 clicking cases consented to participate, providing a response rate of 85.2% and 21.9%, respectively. These contributed to a general response rate of 50.7%. Thirteen locking patients were excluded from data analysis due to their appearing with intermittent lock of the TMJ. The final sample included 55 cases. Of these patients, forty-four (80.0%, 95% CI: 69.4%–90.6%) were female. The participants' age ranged from 15.5 to 69.7 years and the mean age of female and male subjects was 39.7±18.1 years and 30.8±12.1 years, individually. Thirty-nine (70.9%, 95% CI: 58.9%–82.9%) and 16 (29.1%, 95% CI: 17.1%, 41.1%) cases were separately diagnosed with closed lock and TMJ clicking (Table 1).

Two alleles of the ANKH-OR polymorphism were identified, including TCGCCCCG (Allele-1) and TCGCCCCGTCGCCCCG (Allele-2) located in the putative 5′-noncoding region (Figure 2: B–D). According to the combinations of the alleles, there were 7 (12.7%) Allele-1 homozygotes (Genotype 1/1), 23 (41.8%) Allele-2 homozygotes (Genotype 2/2) and 25 (45.5%) Allele-1/Allele-2 heterozygotes (Genotype 1/2) in this sample. Two alleles of the ANKH-TR novel polymorphism were detected in the promoter region, including 7 (Allele-7) and 8 (Allele-8) copies of GGC repeats, respectively (Figure 2: E–G). Combinations of these alleles contributed to 8 (14.5%) Allele-7 homozygotes (Genotype 7/7), 19 (34.6%) Allele-8 homozygotes (Genotype 8/8) and 28 (50.9%) Allele-7/Allele-8 heterozygotes (Genotype 7/8). According to the above, thirty (54.5%, 95% CI: 41.4%–67.7%) ANKH-OR and 27 (49.1%, 95% CI: 35.9%–62.3%) ANKH-TR homozygotes were identified.

Statistically significant variables in the univariate analysis included ANKH-OR ($p = 0.005$, OR = 6.0, 95% CI 1.6–22.3), ANKH-TR ($p = 0.090$, OR = 2.9, 95% CI 0.8–9.8), gender ($p = 0.038$, OR = 0.3, 95% CI 0.1–0.96) and age ($p = 0.003$, OR = 2.2, 95% CI 1.3–3.7). In the multivariate regression model, participants that were ANKH-OR homozygotes (Genotype 1/1 or Genotype 2/2) showed a higher risk of TMJ closed lock than those who were ANKH-OR heterozygotes (Genotype 1/2) ($p = 0.011$, OR = 7.7, 95% CI 1.6–36.5) (Table 1). With the sample size used and a two-sided significance level at 5%, the explanatory power of the test was 0.83, which indicated an adequate statistical power [28]. Older patients more likely sustained closed lock ($p = 0.005$, OR = 2.4, 95% CI 1.3–4.3) (Table 1). Gender and genotypes of ANKH-TR polymorphisms were not related to the type of TMJ internal derangement ($p \geq 0.130$) (Table 1).